

# Advanced Exergy Analysis of an Acid Gas Removal Plant to Explore Operation Improvement Potential toward Cleaner Production

Mohamad Mohamadi-Baghmolaei,\* Abdollah Hajizadeh, Sohrab Zendehboudi,\* Xili Duan, and Hodjat Shiri

Cite This: *Energy Fuels* 2021, 35, 9570–9588

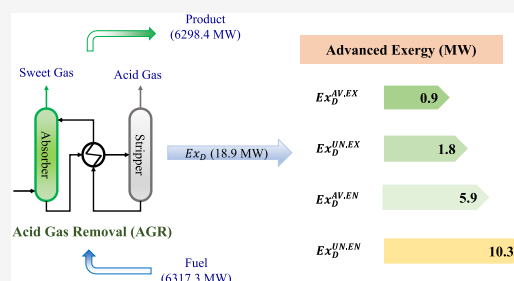
Read Online

ACCESS |

Metrics & More

Article Recommendations

**ABSTRACT:** This research aims to conduct an integrated energy and exergy evaluation of an acid gas recovery (AGR) plant. An effective simulation platform is developed and linked to a thermodynamic modeling approach. A newly developed amine blend, composed of methyl-di-ethanolamine (MDEA), di-ethanolamine (DEA), and piperazine (PZ), is utilized to absorb the acid gases. Based on the classical energy analysis, an energy loss of 70.79 MW and an energy efficiency of 90.29% are attained for each process component. Conventional exergy analysis is then conducted, and the sources of irreversibility are identified. The postprocessing is performed on the conventional exergy evaluation results using an advanced exergy method, to obtain a more realistic insight into the system's energy/exergy performance. It is concluded that stripper and absorber account for the maximum exergy destructions of 8.15 and 7.55 MW, respectively; this shows significant potential for operation improvement in these two key equipment. Also, it is concluded that 5.47 and 4.92 MW unavoidable exergy destructions occur in the stripper and absorber, respectively, which cannot be prevented. It is found from the advanced exergy analysis that the absorber, stripper, and heat exchanger with the greatest recoverable exergy amount (e.g., exergy rehabilitation ratio) exhibit substantial operation enhancement capability in comparison to the other process equipment. The overall exergy efficiency of the entire system is enhanced from 99.70 to 99.90%, when the technological constraints are abolished and the ideal condition governs. The results of avoidable/endogenous exergy destruction reveal high potential of the absorber (2.58 MW), stripper (2.18 MW), heat exchanger (0.74 MW), and valve (0.19 MW) in terms of operation improvement compared to the other process components. Based on the environmental analysis, a large amount of CO<sub>2</sub> emission (22.12 ton·day<sup>-1</sup>) can be prevented, when the process components are technologically upgraded.



## 1. INTRODUCTION

Natural gas is recognized as an environmentally clean fuel compared to conventional fossil fuels, such as coal and oil. Among fossil fuels, natural gas contains the lowest amount of carbon per unit of mass. Natural gas combustion produces less sulfur dioxide, carbon dioxide, and nitrous oxide. Hence, it emits a lower amount of greenhouse gases (GHGs) into the atmosphere.<sup>1</sup> For instance, methane combustion generally results in generating substantially lower amounts of carbon dioxide (CO<sub>2</sub>) compared to conventional fossil fuels (e.g., 30 and 43% lower than oil and coal, respectively).<sup>2</sup> Thus, natural gas (e.g., methane) is reputed as the cleanest hydrocarbon fuel. Also, natural gas is a favorable energy supplier because of its remarkable heating value per unit mass (21520 BTU/lbm).<sup>2</sup> In addition, the easy transportation and storage of natural gas introduce it as a key energy supplier source in the commercial, industrial, and household sectors (23.8% energy consumption worldwide).<sup>3</sup> The shift from conventional fossil fuels to natural gas has been accelerated since the last decade and will continue for the next decade. It is predicted that natural gas

consumption can exceed crude oil consumption between 2020 and 2030.<sup>4,5</sup> Based on the International Energy Agency (IEA) report, fossil fuels will be still the leading energy resource for the next 20 years (e.g., almost 77% of the total energy) in 2040, and the demand for natural gas is estimated to experience the fastest growth rate among fuel resources.<sup>6</sup>

Typically, natural gas contains sulfuric components, such as mercaptans and H<sub>2</sub>S, along with various amounts of CO<sub>2</sub>. Removing the impurities from natural gas is of great importance, considering safety, environmental, and commercial prospects. For example, the impurities can cause corrosion in gas transportation pipelines, causing an economic burden; they can also threaten human health and safety.<sup>7,8</sup> In fact, the

Received: February 22, 2021

Revised: April 6, 2021

Published: May 17, 2021



maximum allowable  $\text{H}_2\text{S}$ ,  $\text{CO}_2$ , and total mercaptans should not surpass 2–4 ppm, 2 vol %, and 5–30 ppm, respectively, to prevent the corrosion in the facilities of gas processing, transportation, and storage.<sup>9,10</sup> On the other hand,  $\text{CO}_2$  as the main contributor of GHGs leads to global warming and significantly reduces the performance of production, transportation, and storage sections.<sup>11</sup> In addition, the  $\text{CO}_2$  content substantially lowers the gas heating value that negatively impacts the price and trading markets. Note that in the United States, above 40% of natural gas resources account for the sour gas; the sour gas content would be more significant for the Middle Eastern countries, where gigantic natural gas reserves are located.<sup>12</sup>

Several methods are available to remove the natural gas impurities, including chemical/physical absorption, the adsorption process via activated carbon, separation with cryogenic distillation, and use of solid/liquid membranes.<sup>13,14</sup> Among all, acid gas removal by alkanolamines is the most widely accepted technique, and most likely, it will remain the most dominant treatment process for the near future.<sup>15</sup> The chemical absorption with alkanolamines is promising for the high removal degree, with acceptable operation costs.<sup>16</sup> Various alkanolamines such as *n*-methyl-di-ethanolamine (MDEA), mono-ethanolamine (MEA), di-ethanolamine (DEA), and di-*iso*-propanolamine (DIPA) are frequently employed in commercial plants with a high removal efficiency. In general, MEA, a primary amine type, is more preferable for industrial gas purification; it is known as the benchmark for other newly developed amine solvents.<sup>17</sup> High gas loading and fast reaction rate are the important benefits of MEA in acid gas removal (AGR) processes. Despite the mentioned advantages, huge requirement of regeneration energy, formation of irreversible and unfavorable products with sulfuric content substances, such as carbon sulfide (COS) and carbon disulfide ( $\text{CS}_2$ ), and being extremely corrosive for high gas loading motivate researchers and engineers to examine other alkanolamines with less environmental concerns and higher economic benefits.<sup>18,19</sup> Remarkable gas absorption and relatively lower regeneration energy are considered as the benefits for other commercialized amines (e.g., MDEA, DEA, and DIPA); however, they suffer from the low to moderate reaction rates with  $\text{CO}_2$ .<sup>20</sup> Besides amines, piperazine (PZ) in the category of cyclic diamines has attracted researchers' attention and emerged as a desired benchmark/solvent for the  $\text{CO}_2$  capture process. PZ is less volatile than MEA and has resistance to thermal degradation. It is also known for fast kinetics.<sup>21</sup> Although amine-based mixtures/solvents are widely used for  $\text{CO}_2$  capture and gas treatment in small to industrial scales, careful attention should be paid to amine degradation products and amine solvent emissions. Indeed, solvent degradation reduces the  $\text{CO}_2$  removal extent, and the additional fresh amine should be introduced to the process. The process equipment is also prone to corrosion and other operational problems, such as foaming.<sup>22</sup> The degradation of amine-based solutions can cause direct environmental impact when released into the air along with the flue gas.<sup>23</sup> Therefore, environmental assessment and solvent optimization are of primary importance to amine-based units.

Typical amine plant configurations need considerable thermal energy in the regeneration section. Several research studies have been conducted to propose new process approaches or efficient amine blends that satisfy both market demand and minimum energy utilization.<sup>24,25</sup> Moioli et al.<sup>26</sup>

studied the energy optimization in an AGR plant. An energy-saving strategy was proposed based on the sensitivity analysis of operating parameters and configuration modification of the plant. The best scenario was chosen in terms of energy requirement in which an acid-gas-rich stream and optimal  $\text{CO}_2$  recovery were achieved. Aromada and Øi<sup>27</sup> conducted a research study with the goal of heat demand reduction in the stripper section. They evaluated alternative process configurations and various operating parameters/conditions to find a cost-efficient scenario. The possible modifications/alternatives were vapor recompression alone and combination of vapor recompression and split-stream approaches to separate 85%  $\text{CO}_2$  from the exhaust gas. Their results revealed that the optimal scenario would be the vapor recompression case, which includes 9 and 20 stages for the stripper and absorber, respectively; however, the cost optimization analysis had a different outcome. The discrepancy between the energy and cost optimization approaches suggests a more comprehensive optimization method. High energy requirement associated with gas sweetening plants, in particular, regeneration energy of the desorption process, is the main concern for new and existing units. To address this concern, Hatmi et al.<sup>28</sup> investigated two strategies, including lean vapor compression (LVC) and rich vapor compression (RVC), to mitigate the energy use of the amine scrubbing plant. The proposed strategies were implemented on two AGR plants working with MDEA and MDEA–PZ solvents. The LVC technique was more efficient since it offered a 40–50% reduction in the reboiler heat duty, while another method (RVC) could save up to 10–11% heat duty. Another common approach for attaining a less energy-intensive amine scrubbing plant is the use of new amine blends; the plant specifications need to be adopted upon a change in the solvent. For instance, Law et al.<sup>29</sup> made an effort to obtain an optimal MEA–MDEA amine blend in terms of lowest reboiler heat duty and highest  $\text{CO}_2$  recovery. Their study highlighted the superiority of the MEA–MDEA blend compared to stand-alone MEA. According to a simulation study on the Argentinian gas sweetening plant, approximately 50% decrease in the energy waste and also the heat duty cost was noted for the best case. As mentioned earlier, gas sweetening plants are suffering from massive reboiler duty and its associated energy loss. The energy requirement in the regeneration section can be reduced up to 48%.<sup>30</sup> The energy performance enhancement of the AGR unit was also investigated by Abd et al.<sup>31</sup> The intensive energy consumption in the amine regeneration process was evaluated while utilizing MDEA and MDEA–PZ blend. A parametric sensitivity evaluation was performed to analyze the impact of various operating factors such as the absorber and stripper pressures, amine rate, reflux ratio, solvent concentration, and acid gas concentration on the required regeneration energy. The simulation outputs revealed that the MDEA–PZ mixture has a higher heat of absorption than MDEA. Also, a considerable amount of energy was required for both amine systems upon an increase in the absorber pressure.<sup>28</sup>

A unique tool to quantitatively detect the irreversibility is exergy evaluation. This energy analysis method is a thermodynamic modeling framework that has been commonly applied to enhance the energy performance of industrial units/plants in the past few decades.<sup>8,32–34</sup> Exergy is simply described as the highest available work, achieved from an energy system. Exergy evaluation considers all vital thermodynamic and process factors of energy stream's components, such

as pressure, temperature, and composition. Indeed, exergy evaluation measures the thermodynamic lost work and process inefficiency in a desired energy system.<sup>35</sup>

The exergy analysis has received wide acceptance among researchers and engineers over the last two decades. There are several research studies in the published literature that focus on the exergy assessment of CO<sub>2</sub> capture through absorption, but less attention has been paid to the exergy analysis of AGR plants that involve high-pressure/-temperature natural gas streams.<sup>36–38</sup> For example, Banat et al.<sup>39</sup> performed exergy evaluation in a gas sweetening plant. The exergy destruction of AGR unit equipment was calculated, and the corresponding exergy efficiencies were determined. The absorber had the highest contribution in exergy destruction (45%) among all of the process components, followed by the air cooler (23%). Their study reports the irreversibility sources and the exergy loss of each component; an energy optimization strategy was not proposed in their work. The exergy analysis is more beneficial when an energy/exergy minimization strategy is employed. An exergy evaluation was conducted on an Iranian AGR unit located in Khangiran gas treatment unit.<sup>40</sup> In this research, the application of mixed MDEA-Sulfinol versus MDEA was analyzed, and the superiority of the blending solvent was confirmed through different test cases. The total exergy efficiency of the blended amines outperformed the MDEA case, significantly. Moreover, the reboiler heat duty was reduced substantially for the mixed amine case. The use of different amine combinations to meet the lowest energy consumption seems promising such that it has potential to lower the operational costs, energy loss, and environmental hazards. The research conducted by Mohamadi-Baghmolaei et al.<sup>35</sup> showed a significant decrease in the cost and energy consumption when the blended MDEA–DEA was employed; approximately 11.6 MW energy units and 14% operation costs were saved at the optimal condition. The results indicated that the stripper and absorber account for the greatest exergy destruction because of the considerable exergy/energy loss in the reboiler and the endothermic reactions in the absorber, respectively.

Recently, the role of natural gas in cleaner and sustainable energy production has been considerably highlighted in several regions across the world. Gas refinery is a high-energy-demand industry, which can lead to substantial environmental concerns (e.g., global warming), along with economic impacts. Therefore, employing energy assessment techniques, such as exergy evaluation, can offer both environmental and economic benefits. Exergy prospects of the heat exchanger systems of a gas refinery were explored by Mehdizadeh-Fard and Pourfayaz.<sup>41</sup> It was concluded that the entire exergy performance of the heat exchanger systems can be improved from 62.8% up to 84.2%. A good instance of cleaner production in the natural gas industry is flare gas recovery. Hajizadeh et al.<sup>42</sup> examined different scenarios to benefit the gas refinery in terms of CO<sub>2</sub>, SO<sub>2</sub>, and SO<sub>3</sub> content reduction while producing liquefied petroleum gas (LPG) and liquefied condensate products. Cleaner production and energy assessment of natural gas production was investigated by Rocco et al.<sup>43</sup> Their research was based on two methods, namely, dual-pressure low-temperature distillation (DPD) and conventional chemical absorption. The results revealed that DPD requires a lower-energy scenario compared to chemical absorption. Additionally, DPD showed higher performance for liquefied natural gas (LNG) production and natural gas purification. To satisfy both

supply–demand and the environmental concerns, coal-based synthesized natural gas (SNG) and shale gas have been found as promising energy resources. A detailed research work was conducted by Zeng et al.<sup>44</sup> to investigate these two energy suppliers through life cycle assessment (LCA) and technoeconomic studies, in China. The results of the LCA assessment for the shale gas production showed that water consumption and GHG emissions are much lower than those from SNG. Moreover, it was concluded that China should pay special attention to the shale gas and consequently slow down the expansion rate of SNG. Another demonstration of cleaner production from natural gas products/byproducts is hydrodesulfurization of LPG, which was conducted by Safari and Vesali-Naseh.<sup>45</sup> The optimization plan was set to minimize the cost of energy and hydrogen consumption needed for converting sulfur impurities into hydrogen sulfide. The optimization results demonstrated the benefits of hydrodesulfurization, for example, production of low-sulfur-content LPG with zero carbon emission and zero water contamination. Converting hydrogen sulfide into elemental sulfur can be considered as the last step of sustainable and cleaner production in gas refineries. In addition to the environmental asset, the elemental sulfur can be easily collected in bulk scale with considerable economic profits. In this regard, Hashemi et al.<sup>46</sup> explored the energy and exergy efficiency of a sulfur recovery unit. Based on their research, waste heat boiler and reaction furnace were the main exergy destruction sources.

To our knowledge, most of the reported exergy analyses on gas sweetening plants involve conventional exergy. Hence, a more sophisticated exergy evaluation is required to obtain comprehensive knowledge on the amount and variations of exergy and energy of various components/units in gas sweetening plants. This study presents an advanced exergy analysis for the first time, as a feasible/practical platform, for energy/exergy evaluation of gas sweetening plants. A real case study is selected, and the utilization of the novel MDEA–DEA–PZ blends is examined through conducting advanced exergy evaluation. The current study is intended to find the irreversibility amount that can be avoided and determine the contribution of internal and external exergy destructions of each process component. Additionally, the current study covers the knowledge gap, existed in cleaner production of natural gas from sour gas, through advanced exergy analysis. Indeed, previous research investigations paid less attention to the advanced exergy analysis of CO<sub>2</sub> capture, and no research work can be found on the advanced exergy assessment of AGR units using chemical absorption. Advanced exergy analysis explores a more realistic understanding of the process exergy so that the behavior of chemical absorption-based AGR can be interpreted with more logical justifications. The advanced exergy analysis is capable of splitting the recoverable/avoidable exergy destruction considering the current technological limitations and equipment costs. Such a strategy can effectively improve the operation performance and assist in designing practical optimization schemes. The conventional exergy analysis only identifies the energy quality and is not able to identify the primary sources of irreversibility and the actual potential of the equipment improvement. The major contribution of this work would be the precise estimation of the avoided CO<sub>2</sub> emissions through performing advanced exergy analysis. This research also offers an effective approach for H<sub>2</sub>S and CO<sub>2</sub> separation from natural gas with the use of newly introduced amine blends. Such an information would

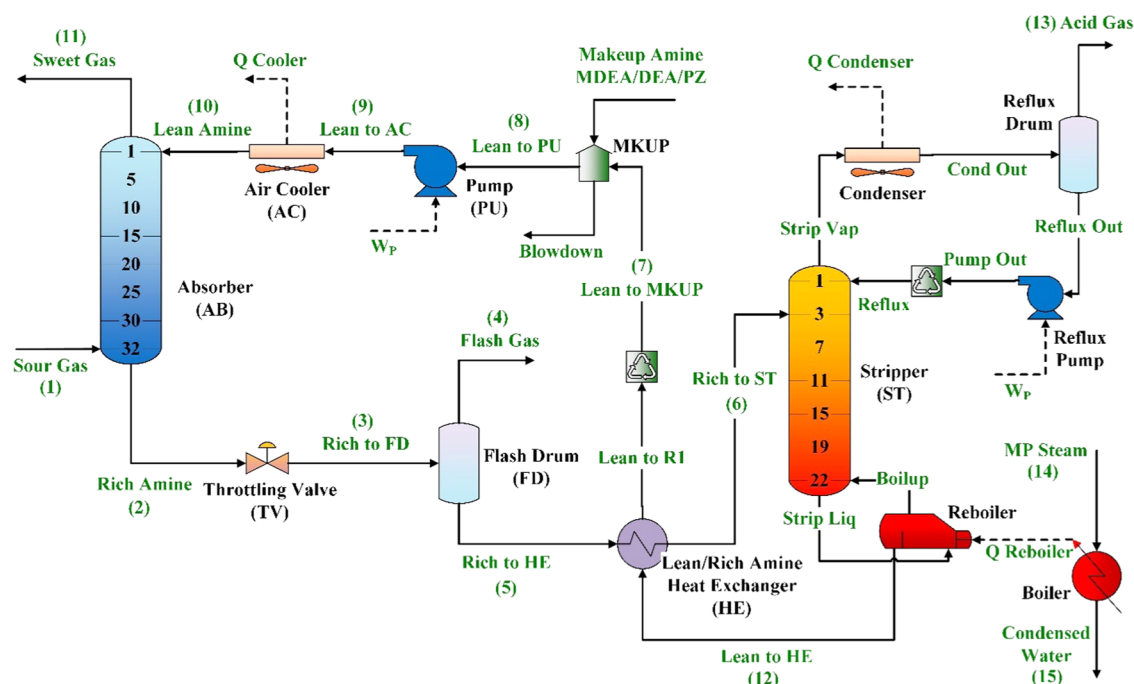


**Figure 1.** Simple schematic of the AGR unit in FJGRC.

Table 1. Main Specifications of the Absorber and Stripper<sup>35</sup>

parameter	absorber	stripper
calculation type	TSWEET kinetics	TSWEET alternate stripper
stages	32	22
stage type	round valve tray	round valve tray
feed stage	1: lean in, 32: sour gas	3: rich in
column diameter (m)	3.7	3.3
height (m)	25.5	21.6
design pressure (bar)	90.0	4.0
operating pressure (bar)	78.1	1.6
pressure drop (bar)	0.57	0.2
design temperature (K)	395.2	424.2

assist energy decision makers to introduce (and select) the practical strategies for enhancing the energy efficiency of entire thermal systems.

It worth noting that the MDEA–DEA–PZ blends have not been practically employed in the large-scale plants. Having PZ as a part of an amine blend requires introducing the standard chemical exergy of newly formed ions, dissolved in the amine solution. Hence, real components (e.g., molecular and ionic components) instead of the apparent molecules are employed in this study. The reliable exergy analysis should be performed based on the real components to lower possible errors due to the use of the apparent components. To validate the simulation phase, the laboratory data collected from an Iranian gas refinery, Fajr-e-Jam Gas Refining Company (FJGRC), are utilized to check the validity of the modeling results.

The rest of this manuscript is structured as follows: process description and reaction mechanisms are found in [Section 2](#). The thermodynamic modeling and methodology parts, involving conventional and advanced thermodynamic concepts, are given in [Sections 3](#) and [4](#). [Section 5](#) contains the results and discussion on the classical energy analysis, and conventional and advanced exergy evaluation. At the end, the

important outcomes of the current study are summarized in [Section 6](#).

## 2. THEORY AND BACKGROUND

This section presents process description and main mechanisms/reactions of acid gas absorption by amine solvent.

**2.1. Process Description.** This study aims to evaluate the energy/exergy efficiency of the AGR unit of the FJGRC, an Iranian gas refinery located in Bushehr province.<sup>35</sup> This refinery receives approximately 100 million standard cubic meters per day (MMSCMD) of sour natural gas, divided into eight trains. The acid gas concentrations of the inflow natural gas stream are considerably greater than the standard limits. This refinery is responsible to capture approximately 6.25 ton·h<sup>-1</sup> H<sub>2</sub>S and 139.21 ton·h<sup>-1</sup> CO<sub>2</sub>. The AGR units, operating with amine solvent, are typically composed of a stripper, an absorber, an amine heat exchanger, an amine pump, a condenser, and an electrical air cooler.<sup>47</sup> The acid gas removal mainly occurs in the absorption column, in which the sour gas and the lean amine enter the column, from the bottom and top parts, respectively. Sweet gas is thus produced from the top side of the column. Throughout the absorption process, the concentration of sour gas in the lean amine increases due to



Table 2. Sour Gas Feed and Lean Amine Specifications

stream	parameter	value	stream	parameter	value
sour gas	flow rate (MMSCMD)	14.94	lean amine	flow rate (SCM/h)	287.83
	temperature (K)	321.2		temperature (K)	328.2
	pressure (bar)	78.7		pressure (bar)	78.1
sour gas composition	N <sub>2</sub> (mol %)	4.97	lean amine composition	MDEA (wt %)	32
	H <sub>2</sub> S (ppm)	1032.93		DEA (wt %)	5.6
	CO <sub>2</sub> (mol %)	1.84		PZ (wt %)	1.96
	CH <sub>4</sub> (mol %)	86.49		acid gas loading (mole acid gas/mole amine)	0.014
	C <sub>2</sub> H <sub>6</sub> (mol %)	4.13	steam	temperature (K)	420.8
	C <sub>3</sub> H <sub>8</sub> (mol %)	1.15		pressure (bar)	4.5
	I-C <sub>4</sub> H <sub>10</sub> (mol %)	0.23			
	N-C <sub>4</sub> H <sub>10</sub> (mol %)	0.34			
	I-C <sub>5</sub> H <sub>12</sub> (mol %)	0.17			
	N-C <sub>5</sub> H <sub>12</sub> (mol %)	0.12			
	N-C <sub>6</sub> H <sub>14</sub> (mol %)	0.17			
	N-C <sub>7</sub> H <sub>16</sub> (mol %)	0.29			

the sour gas solubility in the amine; hence, the regeneration section is needed to provide fresh amine for the process. The rich amine stream leaving the absorber is directed to the stripper column. Figure 1 demonstrates a typical schematic of the AGR unit. The absorber, which has a 3.7 m diameter, is equipped with 32 valve trays. The rich amine solution is sent to the throttling valve to reduce its pressure. Generally, the low-pressure stream is thermodynamically at the two-phase state. To separate the gas and liquid phases, a flash drum is employed. The gas-phase so-called flash gas is discharged from the flash drum. The flash gas mostly includes hydrocarbon gases. The low-pressure liquid stream is received by the amine exchanger to reach a higher temperature by the lean amine stream leaving the stripper from the bottom side. Then, the preheated rich amine is linked to the third stage of the stripper column. The stripper consists of 22 valve trays. The rich amine is regenerated through the stripper and steam reboiler. The stripper and absorber column are two essential equipment of the chemical solvent-based AGR units. Table 1 presents the specifications of the absorber and stripper.

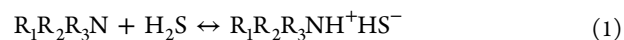
The removed acid gas from the stripper, also known as the distilled product, is delivered to the incinerators. The stripper bottom stream (i.e., lean amine) is cooled down using an amine heat exchanger, pressurized to the absorption pressure, and finally cooled using an air cooler before entering the first stage of the absorber.

The compositions of sour gas feed and amine streams as well as other key operational characteristics of the AGR unit are tabulated in Table 2.

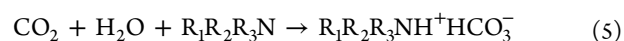
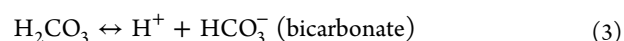
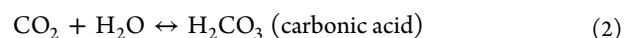
**2.2. Reaction Mechanisms.** The concentration of acidic components in the natural gas needs to be decreased to meet the gas refinery standard specifications and become favorable for further usage and transportation. In this study, MDEA–DEA–PZ blend is employed to absorb the sour gases from the natural gas feed stream. MDEA and DEA are commonly utilized in gas sweetening plants, whereas PZ is mainly used as the promoter for increasing absorption rate.<sup>48,49</sup> MDEA has a high potential to react with H<sub>2</sub>S, in particular, for the cases with a high CO<sub>2</sub>-to-H<sub>2</sub>S ratio. The substantial H<sub>2</sub>S selectivity suggests MDEA as a proper candidate to be utilized in acid gas absorption processes.<sup>17</sup> It should be noted that MDEA is only useful to capture bulk CO<sub>2</sub>.<sup>50,51</sup> Also, DEA as the secondary amine has a remarkable tendency to absorb both H<sub>2</sub>S and CO<sub>2</sub>.<sup>51</sup> On the other hand, PZ with a volatility similar to MEA

exhibits faster kinetics and higher loading capacity (e.g., twice), while it is less prone to oxidation and thermal degradation.<sup>49</sup> Thus, the use of MDEA–DEA–PZ blend can take the advantages of each individual substance.

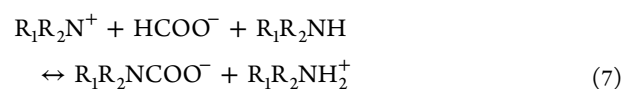
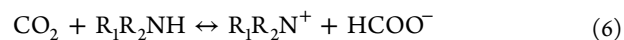
In general, the exothermic reaction occurs between acidic components and amine solution. Despite the structural differences between various amine types, H<sub>2</sub>S reacts with amine by transmitting a direct proton to yield amine hydrosulfide as follows<sup>52</sup>



The reaction of amine solution with CO<sub>2</sub> is more complicated, compared to H<sub>2</sub>S. Various mechanisms are involved in the absorption process. As the first mechanism, CO<sub>2</sub> reacts with H<sub>2</sub>O through the hydrolysis reaction to produce carbonic acid. Then, the bicarbonate is formed by slow dissociation of carbonic acid. Finally, the released proton would react with the amine, based on the following reactions<sup>50,52</sup>



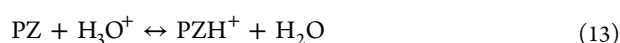
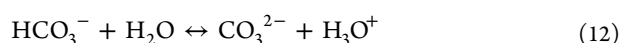
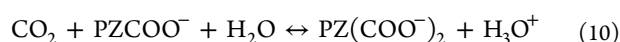
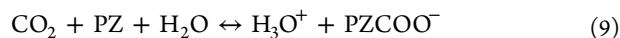
All types of alkanolamines obey the similar mechanisms, but they might have different reaction rates. The second CO<sub>2</sub> reaction mechanism often occurs while dealing with the primary and secondary amines, as shown below<sup>40,42</sup>



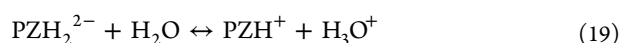
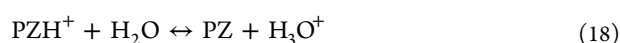
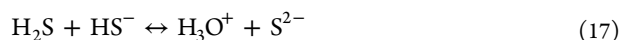
The occurrence of the second important mechanism relies on the abundance of the hydrogen molecule in the amine molecule.<sup>50</sup> The so-called carbamate formation (i.e., the second mechanism) is controlled kinetically and may happen along with the first mechanism simultaneously. These two mechanisms should be taken into account in modeling and

simulation studies when alkanolamines are involved in the absorption process.

The primary and secondary amines react with CO<sub>2</sub> through the zwitterion reaction mechanism, initially introduced by Caplow.<sup>53</sup> The similar mechanism can be assumed for the aqueous PZ reaction with CO<sub>2</sub>.<sup>54</sup> According to this mechanism, zwitterion ion (PZH<sup>+</sup> COO<sup>-</sup>) toward deprotonation with a base (i.e., OH<sup>-</sup>) is produced, and eventually it leads to the formation of the piperazine carbamate (PZCOO<sup>-</sup>) along with protonated PZ.<sup>55</sup> The absorption of CO<sub>2</sub> into the aqueous PZ is kinetically controlled by the generation of piperazine carbamate as well as piperazine dicarbamate, based on the following reactions<sup>56,57</sup>



H<sub>2</sub>O reacts with PZ through an acid–base buffer mechanism. Thus, one can present the main reactions as follows<sup>58</sup>



More information on the theory and mechanisms of the absorption process can be found in a research work by Mohamadi-Baghmolaei et al.<sup>35</sup>

### 3. THERMODYNAMIC MODELING

The energy balance is a traditional technique to determine the process effectiveness of a thermal system. The energy balance takes all types of energy equivalent, regardless of energy quality. In this method, the performance criterion, energy loss, and inherent system irreversibility are not taken into account. The simultaneous application of the first and second laws of thermodynamics provides a practical tool (e.g., exergy evaluation) to explore the irreversibility of thermal systems.<sup>35</sup> Exergy is known as the highest useful thermodynamic work that can be attained from any thermal system.<sup>8,32</sup> Exergy indicates the available work that can be obtained from a system with specific thermophysical properties, and a reference environment.<sup>8</sup> Exergy analysis enables energy engineers to evaluate the exergy changes caused by thermodynamic imperfection of a thermal/chemical process.<sup>33</sup> Unlike the energy conservation law, exergy is not conserved. In fact, the exergy is destroyed in a system, which is referred by exergy destruction/loss.<sup>30,49</sup> The exergy analysis determines the location and the quantity of the exergy destruction. To achieve the exergy balance of a thermodynamic system, the energy and mass balances on the basis of the first and second laws of

thermodynamics should be considered.<sup>59</sup> The exergy equity of a control volume is given by the following expression

$$\frac{d(E)}{dt} = \sum_i \left(1 - \frac{T_0}{T_i}\right) \dot{Q}_i - \dot{E}_{\text{work}} + \sum_i \dot{E}_{\text{in},i} - \sum_e \dot{E}_{\text{out},e} - \dot{E}_D \quad (20)$$

where  $E$  shows the amount of exergy;  $t$  denotes the time;  $T_0$  and  $T_i$  are the ambient air temperature and the surrounding boundary temperature, respectively;  $\dot{Q}_i$  refers to the heat that crosses the control volume boundary;  $\dot{E}_{\text{work}}$  introduces the mechanical and electrical works;  $\dot{E}_{\text{in},i}$  and  $\dot{E}_{\text{out},e}$  stand for the exergy rate of the input and output streams, respectively; Also,  $\dot{E}_D$  resembles the exergy destruction flow. Note that both of the physical and chemical exergy terms are included in the exergy rates (e.g.,  $\dot{E}_{\text{in},i}$  and  $\dot{E}_{\text{out},e}$ ).

**3.1. Physical Exergy.** The physical exergy is described as the maximum thermodynamic work that can be achieved from the interaction of control volume with a certain state (e.g., temperature, pressure, potential energy, and velocity) and the reference state of the surrounding. The physical exergy ( $ex_{\text{ph}}$ ) is expressed as follows<sup>8</sup>

$$ex_{\text{ph}} = (h - h_0) - T_0(s - s_0) + \frac{V^2}{2} + gz \quad (21)$$

In eq 21,  $V$ ,  $g$ ,  $h$ ,  $s$ , and  $z$  refer to the velocity (m·s<sup>-1</sup>), acceleration due to the gravity (m·s<sup>-2</sup>), enthalpy (J·mol<sup>-1</sup>), entropy (J·mol<sup>-1</sup>·K<sup>-1</sup>), and height (m), respectively. Also, zero (0) subscript denotes the surrounding condition. For practical cases, the kinetic and potential terms are generally ignored, compared to high magnitudes of enthalpy, entropy, and chemical exergy content of the substances.

**3.2. Chemical Exergy.** The minimum work required to form a substance at the ambient condition, from the stable components in the reference environment, is defined as chemical exergy.<sup>60</sup> The chemical exergy is a criterion of energy/exergy content of a substance with respect to its stable/common reference composition in the environment state. To obtain the chemical exergy in the nonequilibrium environment, the components' standard chemical exergy obtained from the standard exergy of the reference substances should be used.<sup>60</sup> The reference species are the most stable form of species of the reference environment, representing the lowest content of chemical exergy.<sup>61</sup> The ideal gas mixture chemical exergy is computed by the following expression<sup>39</sup>

$$ex_{\text{ch,mix}}^{\text{ig}} = \sum_i y_i ex_{\text{ch},i}^0 + RT_0 \sum_i y_i \ln(y_i) \quad (22)$$

where  $y_i$  is the molar fraction of components in the gas mixture;  $ex_{\text{ch},i}^0$  introduces the component's standard chemical exergy; and  $R$  shows the universal gas constant. Equation 22 can also be used to obtain the chemical exergy of an ideal solution. For nonideal solutions, the chemical exergy calculation depends on the components' standard chemical exergy and their activity coefficients, as shown below<sup>37</sup>

$$ex_{\text{ch,sol}} = \sum_i x_i ex_{\text{ch},i}^0 + RT_0 \sum_i x_i \ln(a_i) \quad (23)$$

where  $x_i$  resembles the molar fraction of liquid components and  $a_i$  expresses the activity of the liquid components. The total chemical exergy of nonideal and ionic solutions, such as

salts and water, can be obtained using the following relationship<sup>61</sup>

$$ex_{ch, sol}^{ionic} = \sum_i n_i (ex_{ch,i}^a + RT_0 \ln(M_i \gamma_i)) + n_w (ex_{ch,w}^0 + RT_0 \ln(x_w \gamma_w)) \quad (24)$$

where  $\gamma_i$ ,  $ex_{ch,i}^a$  and  $M_i$  denote the activity coefficient of components in the solution, the component's standard chemical exergy in the aqueous solution, and the component's molality, respectively. Moreover,  $\gamma_w$ ,  $x_w$ ,  $n_w$ ,  $ex_{ch,w}^0$  and  $n_i$  are the water activity coefficient, water mole fraction, number of moles of water in the solution, standard chemical exergy of water, and the number of component's mole in the solution, respectively. It is worth mentioning that the activity coefficients of the molecular and ionic components, present in the ionic and nonideal solutions, are obtained from Aspen Plus ELECNRTL model. This model calculates these coefficients with high accuracy. It should be noted that the components' standard chemical exergy in the solution ( $ex_{ch,i}^a$ ) is determined by the following expression<sup>33</sup>

$$ex_{ch,i}^a = ex_{ch,i}^0 + \Delta_f G_{aq,i} - \Delta_f G_i^0 \quad (25)$$

where  $\Delta_f G_{aq,i}$  symbolizes the component's formation Gibbs free energy in the solution, and the pure component's formation Gibbs free energy is expressed by  $\Delta_f G_i^0$ . Note that the pure component's Gibbs free energy of formation is typically larger than Gibbs free energy of formation of the components in the solutions. In addition, the pure organic salts' Gibbs free energy is approximately 10 kJ·mol<sup>-1</sup> higher than Gibbs free energy of dissolved salts.<sup>39</sup>

**3.3. Advanced Exergy Analysis.** To improve the system energy performance, the exergy loss/destruction should be reduced as much as possible. It should be emphasized that the thermodynamic inefficiency can only be avoided, relatively. The rest of the imperfections is unavoidable and inevitable. Thus, the practically possible amendments should be applied to the avoidable part of thermodynamic irreversibility. The advanced exergy assessment should focus on the avoidable thermodynamic inefficiency to achieve a better system performance. The component's exergy destruction rate in a thermal system comprises avoidable and unavoidable exergy destructions as shown below<sup>62</sup>

$$\dot{E}_{D,k} = \dot{E}_{D,k}^{AV} + \dot{E}_{D,k}^{UN} \quad (26)$$

where  $\dot{E}_{D,k}^{AV}$  and  $\dot{E}_{D,k}^{UN}$  stand for the  $k^{\text{th}}$  component's avoidable and unavoidable exergy destructions of the, respectively. To find the unavoidable exergy destruction, the correlation between the investment cost and the exergy destruction should be explored well. In general, it is known that the cost and exergy destruction depend on each other. In other words, the investment per product exergy boosts up with enhancing the exergy efficiency.<sup>62</sup> The maximum exergy efficiency is achieved when the investment cost becomes very large (e.g., infinite mathematically). At this condition, the unavoidable exergy destruction per product exergy unit  $\left(\frac{\dot{E}_D}{\dot{E}_P}\right)_k^{UN}$  is obtained.

For practical purposes, the unavoidable exergy destruction per product exergy unit is met by choosing proper thermodynamic criteria that offer the maximum efficiency.<sup>62</sup> Knowing this parameter  $\left(\frac{\dot{E}_D}{\dot{E}_P}\right)_k^{UN}$ , other unknown components such as

unavoidable and avoidable exergy destruction rates ( $\dot{E}_{D,k}^{UN}$  and  $\dot{E}_{D,k}^{AV}$ ) are found through the following equations<sup>63</sup>

$$\dot{E}_{D,k}^{UN} = \dot{E}_{P,k} \left( \frac{\dot{E}_D}{\dot{E}_P} \right)_k^{UN} \quad (27)$$

$$\dot{E}_{D,k}^{AV} = \dot{E}_D - \dot{E}_{D,k}^{UN} \quad (28)$$

To make the exergy evaluation more applicable for energy experts, the interactions between system components should be taken into account. The interactions are calculated and presented by component's endogenous exergy destruction and exogenous exergy destruction as follows<sup>63</sup>

$$\dot{E}_{D,k} = \dot{E}_{D,k}^{EN} + \dot{E}_{D,k}^{EX} \quad (29)$$

where  $\dot{E}_{D,k}^{EN}$  introduces the endogenous exergy destruction and  $\dot{E}_{D,k}^{EX}$  refers to the exogenous exergy destruction. Note that the endogenous exergy destruction is resulted from the interactions in the  $k^{\text{th}}$  component, whereas the exogenous exergy destruction is presented by the rest of overall exergy destruction, described as the irreversibility that takes place in other components of the thermal system. The endogenous exergy destruction can be computed as follows<sup>64</sup>

$$\dot{E}_{D,k}^{EN} = \dot{E}_{P,k}^{ideal} \left( \frac{1}{\varepsilon_k} - 1 \right) \quad (30)$$

where  $\dot{E}_{P,k}^{ideal}$  expresses the product exergy, when all components are under ideal condition, except the  $k^{\text{th}}$  component, and  $\varepsilon_k$  indicates the exergy efficiency, which is discussed later.

A combination of the avoidable/unavoidable concepts and endogenous/exogenous theories provides important applicable terms such as unavoidable-endogenous ( $\dot{E}_{D,k}^{UN,EN}$ ), unavoidable-exogenous ( $\dot{E}_{D,k}^{UN,EX}$ ), avoidable-endogenous ( $\dot{E}_{D,k}^{AV,EN}$ ), and avoidable-exogenous ( $\dot{E}_{D,k}^{AV,EX}$ ). The avoidable-endogenous term refers to the destructions resulted from the system component ( $k^{\text{th}}$ ), while the avoidable-exogenous term addresses the destructions originated from other components.<sup>63</sup> The avoidable-endogenous term can be improved by fundamental enhancement of the entire system as well as increasing efficiency of other process components.<sup>65</sup> The aforementioned parameters are expressed as follows<sup>63</sup>

$$\dot{E}_{D,k}^{UN,EN} = \dot{E}_{P,k}^{EN} \left( \frac{\dot{E}_D}{\dot{E}_P} \right)_k^{UN} \quad (31)$$

$$\dot{E}_{D,k}^{UN,EX} = \dot{E}_{D,k}^{UN} - \dot{E}_{D,k}^{UN,EN} \quad (32)$$

$$\dot{E}_{D,k}^{AV,EN} = \dot{E}_{D,k}^{EN} - \dot{E}_{D,k}^{UN,EN} \quad (33)$$

$$\dot{E}_{D,k}^{AV,EX} = \dot{E}_{D,k}^{EX} - \dot{E}_{D,k}^{UN,EX} \quad (34)$$

As discussed earlier, the term  $\left(\frac{\dot{E}_D}{\dot{E}_P}\right)_k^{UN}$  plays an important role in determining other exergy destruction parameters. The proportion of exergy destruction per product exergy at unavoidable state is also considered for the ratio of unavoidable/endogenous exergy destruction to endogenous product exergy of the  $k^{\text{th}}$  component. Thus, the unavoidable/endogenous exergy destruction for each component is determined. Subtracting the unavoidable/endogenous exergy destruction from unavoidable exergy destruction for each

component then provides the unavoidable/exogenous exergy destruction of the  $k^{\text{th}}$  component. Knowing the endogenous/exogenous exergy destruction terms, one can obtain the avoidable/endogenous and avoidable/exogenous destruction parameters using eqs 33 and 34.

**3.4. Exergy Efficiency.** The  $k^{\text{th}}$  component's exergy efficiency ( $\epsilon$ ) is expressed as the proportion of output to the input exergy rate, as written below<sup>63</sup>

$$\epsilon_k = \frac{\dot{E}_{\text{out},k}}{\dot{E}_{\text{in},k}} = 1 - \frac{\dot{E}_{\text{D},k}}{\dot{E}_{\text{in},k}} \quad (35)$$

A more practical description of exergy efficiency is presented on the basis of the fuel and product exergy concepts. This method relates the exergy efficiency of component  $k$  to the ratio of the exergies of fuel and product of process component  $k$  in an energy conversion system as presented below

$$\epsilon_k = \frac{\dot{E}_{\text{P},k}}{\dot{E}_{\text{F},k}} = 1 - \frac{\dot{E}_{\text{D},k} + \dot{E}_{\text{L},k}}{\dot{E}_{\text{F},k}} \quad (36)$$

where  $\epsilon_k$  denotes the exergy efficiency of the  $k^{\text{th}}$  component;  $\dot{E}_{\text{P},k}$  accounts for the exergy of product/output ( $\text{J}\cdot\text{mol}^{-1}$ );  $\dot{E}_{\text{F},k}$  resembles the exergy of fuel ( $\text{J}\cdot\text{mol}^{-1}$ ); and  $\dot{E}_{\text{L},k}$  and  $\dot{E}_{\text{D},k}$  refer to the exergy loss and exergy destruction of the  $k^{\text{th}}$  component, respectively. The  $k^{\text{th}}$  component's exergy destruction rate is obtained using the following equation<sup>66</sup>

$$\dot{E}_{\text{D},k} = \dot{E}_{\text{F},k} - \dot{E}_{\text{P},k} - \dot{E}_{\text{L},k} \quad (37)$$

It is worth mentioning that the exergy loss can be zero when the temperature of component boundaries is fixed at  $T_0$ .<sup>66</sup> Obtaining the exergy destruction ratio is another vital step in exergy analysis. The so-called exergy destruction ratio ( $y_{\text{D},k}$ ) is described as the proportion of exergy destruction of the  $k^{\text{th}}$  component to the overall fuel supply. The exergy destruction ratio of the  $k^{\text{th}}$  component is presented as follows<sup>67</sup>

$$y_{\text{D},k} = \frac{\dot{E}_{\text{D},k}}{\dot{E}_{\text{F},\text{tot}}} \quad (38)$$

where  $\dot{E}_{\text{F},\text{tot}}$  represents the system fuel supply. The exergy efficiency of the entire system is computed by the following expression<sup>67</sup>

$$\epsilon_{\text{total}} = \frac{\dot{E}_{\text{P},\text{tot}}}{\dot{E}_{\text{F},\text{tot}}} = 1 - \sum_k y_{\text{D},k} - \frac{\dot{E}_{\text{L},\text{tot}}}{\dot{E}_{\text{F},\text{tot}}} \quad (39)$$

In eq 39,  $\epsilon_{\text{total}}$  resembles the total system exergy efficiency;  $\dot{E}_{\text{P},\text{tot}}$  represents the total system product exergy; and  $\dot{E}_{\text{L},\text{tot}}$  introduces the overall exergy loss of the corresponding system. The exergy destruction ratio ( $y_{\text{D},k}^{\text{AV,EN}}$ ) and modified exergy efficiency ( $\epsilon_k^{**}$ ) considering avoidable-endogenous exergy destruction are defined as follows<sup>67</sup>

$$y_{\text{D},k}^{\text{AV,EN}} = \frac{\dot{E}_{\text{D},k}^{\text{AV,EN}}}{\dot{E}_{\text{F},\text{total}}} \quad (40)$$

$$\epsilon_k^{**} = \frac{\dot{E}_{\text{P},k}}{\dot{E}_{\text{F},k} - \dot{E}_{\text{D},k}^{\text{UN}} - \dot{E}_{\text{D},k}^{\text{AV,EX}}} \quad (41)$$

The exergetic fuel depletion ratio ( $\delta_k$ ), exergetic rehabilitation ratio ( $\text{ERR}_k$ ), exergetic productivity ratio ( $\xi_k$ ), and exergetic improvement potential ratio ( $\text{EIP}_k$ ) are the supplementary exergetic parameters in the exergy analysis.<sup>65</sup> They help in the

interpretation and deployment of energy/exergy efficiency of a thermal system. These parameters are expressed as follows<sup>65</sup>

$$\delta_k = \frac{\dot{E}_{\text{D},k}^{\text{UN}} + \dot{E}_{\text{D},k}^{\text{AV,EX}}}{\dot{E}_{\text{F},\text{total}}} \quad (42)$$

$$\text{ERR}_k = \frac{\dot{E}_{\text{D},k} - \dot{E}_{\text{D},k}^{\text{UN}} - \dot{E}_{\text{D},k}^{\text{AV,EX}}}{\dot{E}_{\text{D},\text{total}}} \quad (43)$$

$$\xi_k = \frac{\dot{E}_{\text{D},k}^{\text{UN}} + \dot{E}_{\text{D},k}^{\text{AV,EX}}}{\dot{E}_{\text{P},\text{total}}} \quad (44)$$

$$\text{EIP}_k = \frac{\dot{E}_{\text{D},k}^{\text{UN}} + \dot{E}_{\text{D},k}^{\text{AV,EX}}}{\dot{E}_{\text{F},k}} \quad (45)$$

## 4. METHODOLOGY

The modeling/simulation procedure along with the assumptions are presented in this section. A robust simulation platform that takes into account the real plant operation states is necessary for the exergy evaluation of the gas sweetening unit. Thus, we conduct the simulation part using the ProMax Bryan Research Engineering (BRE) simulation tool version 3.2. This software has been approved to be an excellent choice to simulate gas processing units. Version 3.2 of the software is suitable to simulate the AGR plants operating with PZ solution. Thus, this version is chosen for the case study of the current research that uses a mixture of MDEA, DEA, and PZ.

The simulation platform requires a proper thermodynamic model to precisely predict the chemical/physical properties. In this study, the so-called amine sweetening Soave–Redlich–Kwong (SRK), a built-in thermodynamic package of ProMax BRE, is employed. This property package is an activity coefficient model, which considers the liquid-phase activity coefficients in the equality fugacity equations of multi-component phase equilibria. The SRK equation of state (EOS) is also employed to find the fugacity of the components in the gas phase under equilibrium.

The simulation results are validated using operational data collected from the laboratory. The acidic composition is determined based on characteristic tests conducted in the laboratory of the gas refinery. The  $\text{H}_2\text{S}$  and  $\text{CO}_2$  contents of the sweet gas stream, steam flow rate, and stripper bottom temperature are the set points for the simulation phase. The operation and simulation data are reported in Table 3. The

**Table 3. Comparison of Operation Data and Simulation Outputs**

parameter	operation	simulation	RD%
$\text{H}_2\text{S}$ outlet (ppm)	2.90	2.87	1.03
$\text{CO}_2$ outlet (ppm)	628.0	627.4	0.09
steam flow rate ( $\text{ton}\cdot\text{h}^{-1}$ )	40.58	40.59	0.02
stripper bottom temperature (K)	392.9	393.3	0.10

accuracy and reliability of the simulation results are determined using relative deviation (RD) percentage as follows

$$\text{RD\%} = \frac{|x^{\text{Op}} - x^{\text{Sim}}|}{x^{\text{Op}}} \times 100 \quad (46)$$



Table 4. Assumed Unavoidable and Theoretical States for Various Equipment

component, <i>k</i>	operation cond.	unavoidable cond.	theoretical cond.	ref
PU	$\eta = 0.65$	$\eta = 0.95$	$\eta = 1$	68
TV		$\eta_{\text{is}}^{\text{turbine}} = 0.95$	$\eta_{\text{is}}^{\text{turbine}} = 1$	68
HE	$\Delta T_{\text{min}} = 25.4 \text{ K}$	$\Delta T_{\text{min}} = 5 \text{ K}$	$\Delta T_{\text{min}} = 0 \text{ K}$	69
AC	$\Delta T_{\text{min}} = 20 \text{ K}$	$\Delta T_{\text{min}} = 5 \text{ K}$	$\Delta T_{\text{min}} = 0 \text{ K}$	69
ST	$\Psi_{\text{M}}^{\text{CO}_2\text{H}_2\text{S}} = 1$	$\Psi_{\text{M}}^{\text{CO}_2\text{H}_2\text{S}} = 1.5$	$\Psi_{\text{M}}^{\text{CO}_2\text{H}_2\text{S}} = 1.9$	this study <sup>a</sup>
AB	$\Delta P = 0.57 \text{ bar}$	$\Delta P = 0.05 \text{ bar}$	$\Delta P = 0 \text{ bar, L/G} \rightarrow \text{min}$	38

<sup>a</sup>It should be noted that the Murphree efficiency, as an indicator of the closeness to the equilibrium state on a stage within a stripper column,<sup>70</sup> is employed to specify the unavoidable and theoretical states.

where  $x^{\text{Op}}$  stands for the operation parameter and  $x^{\text{Sim}}$  represents the simulation value.

The pressure, temperature, and molar composition of each stream are introduced into the Aspen Plus V11 with ENRTL thermodynamic model for postprocessing after obtaining the simulation results from the ProMax BRE. Indeed, ProMax BRE is unable to calculate the physical exergy and activity coefficients of newly defined ions. In the next step, the thermodynamic relations are coded with MATLAB R2019a to compute the parameters of classical energy analysis and conventional and advanced exergy approaches. The following procedure is conducted to obtain the energy and exergy parameters:

- The standard chemical exergy for gas and liquid components should be collected from the literature if available. Otherwise, we need to calculate this parameter for the new components (e.g., ions).
- The physical exergy of each stream should be determined considering enthalpy and entropy of each stream.
- The activity coefficient calculated for nonideal solutions should be introduced to the MATLAB R2019a program code.
- The chemical exergy computation is conducted at the reference pressure and temperature. Therefore, it is not affected by the operating pressure and temperature. However, the stream composition is needed to achieve chemical exergy accurately.
- The chemical exergy of the gas and liquid mixtures is obtained by eqs 22 and 23.
- For the ionic solution, first, the standard chemical exergy of the ionic components should be determined by eq 25. Then, the nonideal solution chemical exergy can be obtained using eq 24.
- The amount of total exergy is determined by having the chemical exergy and physical exergy values, which are obtained by using Aspen Plus V11.
- In this step, the exergy destruction values can be calculated based on the relationships between exergy streams shown in Table 7.
- The exergy destruction of every single component and that of the entire system are the feed/input information for the advanced exergy analysis. Equations 27 to 34 introduce the advanced exergy parameters that are essential for postanalysis.
- To find the unavoidable exergy destruction, each process component is individually simulated, considering the unavoidable condition, provided in Table 4. As a result,

$\left(\frac{\dot{E}_D}{\dot{E}_P}\right)_k^{\text{UN}}$  is attained, and correspondingly,  $\dot{E}_{D,k}^{\text{UN}}$  and  $\dot{E}_{D,k}^{\text{AV}}$

are achieved using eqs 27 and 28, respectively.

- The endogenous exergy destruction is calculated based on eq 30. The required term,  $\dot{E}_{P,k}^{\text{ideal}}$ , is determined when all of the process components are operating at the predetermined theoretical state, except the components being assessed. The theoretical state for each process component is provided in Table 4. Once the ideal term,  $\dot{E}_{P,k}^{\text{ideal}}$ , is calculated, the endogenous exergy and exogenous exergy destructions can be computed.
- Finally, the modified exergy efficiency and exergetic parameters can be computed using eqs 40–45.

The assumptions for the theoretical, unavoidable, and operational conditions are presented in Table 4. It is assumed that  $\dot{E}_{D,k}$  is equal to zero; if not possible,  $\dot{E}_{D,k}$  should be at its minimum value to obtain the theoretical state. The presumptions for the unavoidable states are made according to the knowledge of process and operation engineers.

Besides the exergy and energy, the economic and environmental aspects of the AGR unit are evaluated. Another energy evaluation method is also performed with applying the specific energy consumption (SEC) index. The energy consumption, in this study, is described as the energy consumed by the main equipment of the AGR, including stripper, reboiler, air cooler, condenser, and amine pump. Furthermore, the steam reboiler is mostly responsible for the GHG emissions in the AGR unit. The steam is provided for fuel/methane combustion. In this work, the stoichiometric amount of  $\text{CO}_2$  required for combustion reaction can be determined for the environmental assessment. The detailed information on the energy and environmental assessment of the AGR unit can be found in a research study conducted by Mohamadi-Baghmolaei et al.<sup>35</sup> It should be mentioned that the main operational costs such as carbon tax, electricity, and steam costs are incorporated in the economic evaluation of the AGR unit. The costs for the carbon tax and electricity are 25 USD/ (ton of emitted  $\text{CO}_2$ )<sup>71</sup> and 0.067 USD/kWh,<sup>72</sup> respectively. Also, the cost of employed steam is estimated using the latest natural gas cost, 2.48 USD/1000 ft<sup>3</sup>.<sup>72</sup> The electricity consumption in this study includes the electricity usage of the air cooler and amine pump.

## 5. RESULTS AND DISCUSSION

The results and discussion on the conventional energy analysis, classical exergy analysis, and advanced exergy analysis are presented in this section.

**5.1. Energy Analysis.** The classical energy evaluation is conducted using energy balance around every single process component of the AGR unit as well as the entire system. Figure 2 demonstrates the energy loss contributions of the AGR

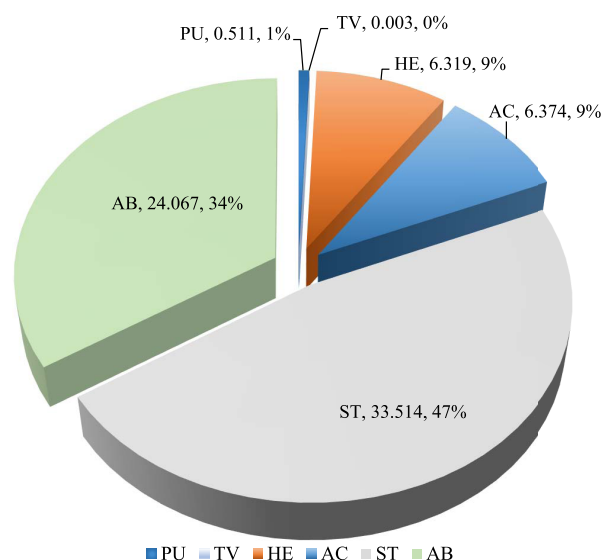


**Figure 2.** Energy loss of various equipment involved in the gas sweetening plant; energy loss values are reported in MW.

equipment. The values of energy efficiency are obtained based on the relationships introduced by Talebizadehsardari et al.<sup>73</sup> The results reveal that the stripper and absorber are responsible for the largest energy losses of 33.51 and 24.07 MW, respectively. The stripper and absorber, respectively, account for 47 and 34% of the total energy loss. The rest of total energy loss belongs to the air cooler and heat exchanger, approximately 18%. These process components are responsible for relatively the same portion of energy loss, 9%. The air cooler has a slightly higher energy loss (6.37 MW) than the heat exchanger (6.32 MW). Other process components exhibit a marginal energy loss, compared to the equipment mentioned earlier.

To determine the energy quality, energy efficiency is employed for each equipment and the entire AGR unit. The breakdown of energy efficiency for the process components of the AGR unit is provided in Figure 3. As seen in Figure 3, the

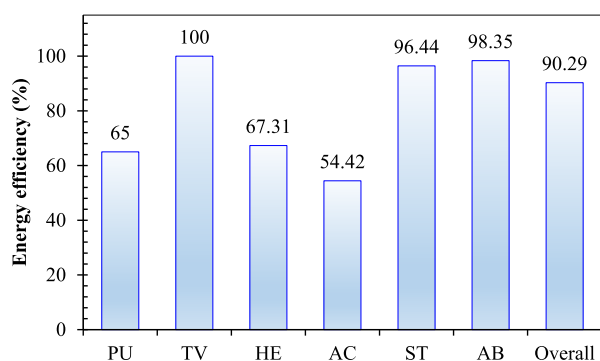


**Figure 3.** Extent of energy performance for the main process equipment of the AGR unit.

highest energy efficiency is achieved for the flash drum and throttling valve with almost a perfect efficiency. The high energy performance is attained, when the source of energy loss is insignificant such as throttling valve and flash drum. It is worth noting that the throttling valve and flash drum are considered as one component package in the energy efficiency calculation. Other process components with a high energy

efficiency are the absorber (98.35%) and stripper (96.44%). Special care should be taken regarding the high energy performance of the absorber and stripper. The high energy performance of these two components is mainly due to the considerable amount of input and output energy streams, compared to the energy loss value. The energy performance of the remaining equipment is as follows: heat exchanger (67.31%), pump (65%), and air cooler (54.42%).

**5.2. Exergy Analysis.** The exergy analysis of gas sweetening plants that include several gas, liquid, and ionic streams is a complicated task. The vital thermodynamic information or parameters such as standard chemical exergy and standard formation Gibbs free energy of gas, liquid, and ionic components, activity coefficients, and gas compressibility factor are required for the exergy assessment. The standard chemical exergy and standard formation Gibbs free energy of ionic components are listed in Table 5. It is worth mentioning

**Table 5.** Thermodynamic Information Needed for the Exergy Calculation of Ionic Components

component	$ex_{ch}^0$ (kJ·mol <sup>-1</sup> )	$g_{fo}$ (kJ·mol <sup>-1</sup> )
H <sub>3</sub> O <sub>(aq)</sub> <sup>+</sup>	32.39	-237.13
HS <sub>(aq)</sub> <sup>-</sup>	817.715	12.08
DEAH <sub>(aq)</sub> <sup>+</sup>	2659.175	-324.72
DEACOO <sub>(aq)</sub> <sup>-</sup>	2733.7	-624.376
MDEAH <sub>(aq)</sub> <sup>+</sup>	3370.365	-259.89
HCO <sub>3(aq)</sub> <sup>-</sup>	16.887	-586.77
PZCOO <sub>(aq)</sub> <sup>-</sup>	2693.649	-214.564
H <sup>+</sup> PZCOO <sub>(aq)</sub> <sup>-</sup>	3236.425	-267.716
CO <sub>3(aq)</sub> <sup>-2</sup>	35.792	-527.81
PZHH <sub>(aq)</sub> <sup>++</sup>	2962.596	60.301
PZH <sub>(aq)</sub> <sup>+</sup>	2953.188	90.9
S <sub>(aq)</sub> <sup>2-</sup>	851.38	85.8
HS <sub>(aq)</sub> <sup>-</sup>	817.715	12.08
OH <sub>(aq)</sub> <sup>-</sup>	32.173	-157.244

that assuming (or considering) the ionic components as apparent molecules in the thermodynamic modeling can cause appreciable inaccuracy, resulting in erroneous outcomes. This research work introduces the required thermodynamic information for calculation of ionic components' chemical exergy, for the first time (see Table 3).

As mentioned earlier, the pressure, temperature, molar flow rates, and magnitudes of exergy flow are needed to perform the classical and/or advanced exergy analysis (see Table 6). The exergy values (e.g., chemical exergy and physical exergy) are obtained through the procedure explained in the thermodynamic section (Section 3).

The conventional exergy evaluation is conducted to obtain the exergy destruction amount and exergy efficiency of process components. It should be noted that the fuel-product approach is used in this research study for calculating the exergy efficiency of each component. The exergy efficiency of the fuel and product streams depends on the operator's desire and the company strategies. In some equipment such as air cooler, the proposed exergy efficiency might not be the same in various studies.

The exergy destruction and efficiency are obtained using the equations provided in Table 7.

The overall fuel and product exergies of the system are 6317.30 and 6298.43 MW, respectively. Also, the calculations show that the total exergy destruction is 18.87 MW. The

Table 6. Key Thermodynamic Characteristics of the Operation State for the Flow Streams

stream no.	temperature (K)	pressure (bar)	flow rate (kmol·h)	physical exergy (MW)	chemical exergy (MW)	total exergy (MW)
1	321.15	78.71	26324.20	73.748	6025.333	6099.081
2	325.65	78.71	11112.90	0.760	919.269	920.029
3	327.20	8.01	11112.90	0.455	910.264	910.719
4	327.21	6.89	18.67	0.024	3.956	3.981
5	327.21	6.89	11094.22	0.424	906.309	906.733
6	367.9	6.79	11094.22	2.034	906.685	908.720
7	352.36	1.46	10537.87	1.308	901.240	902.548
8	351.61	1.46	10738.35	1.293	901.393	902.686
9	353.21	78.34	10738.35	1.737	901.398	903.136
10	328.15	78.14	10738.35	0.793	901.398	902.192
11	342.31	78.14	25949.65	75.636	6211.018	6286.655
12	393.30	1.81	10537.86	4.259	901.379	905.639
13	328.15	1.41	556.18	0.156	8.797	8.953
14	420.81	4.46	2252.88	8.024	5.937	13.962
15	420.81	4.46	2252.88	8.023	0.563	8.586

Table 7. Equations Used to Compute Exergy Destruction and Efficiency of the Equipment

component, <i>k</i>	exergy destruction	exergy efficiency	ref
flash drum (FD)	$\dot{E}_D^{FD} = \dot{E}_3 - (\dot{E}_4 + \dot{E}_5)$	$\varepsilon_{FD} = \frac{\dot{E}_4 + \dot{E}_5}{\dot{E}_3}$	74
pump (PU)	$\dot{E}_D^{PU} = \dot{W}_p + \dot{E}_8 - \dot{E}_9$	$\varepsilon_{PU} = \frac{\dot{E}_9 - \dot{E}_8}{\dot{W}_p}$	73
throttling valve (TV)	$\dot{E}_D^{TV} = \dot{E}_3 - \dot{E}_2$	$\varepsilon_{TV} = \frac{\dot{E}_3}{\dot{E}_2}$	this study
heat exchanger (HE)	$\dot{E}_D^{HE} = \dot{E}_5 + \dot{E}_{12} - (\dot{E}_6 + \dot{E}_7)$	$\varepsilon_{HE} = \frac{\dot{E}_6 - \dot{E}_5}{\dot{E}_{12} - \dot{E}_7}$	75
air cooler (AC)	$\dot{E}_D^{AC} = \dot{W}_{AC} + \dot{E}_9 - \dot{E}_{10}$	$\varepsilon_{AC} = \frac{\dot{E}_{10}}{\dot{W}_{AC} + \dot{E}_9}$	this study
stripper (ST)	$\dot{E}_D^{ST} = \dot{E}_6 + \dot{E}_{14} + \dot{W}_{AC} - (\dot{E}_{12} + \dot{E}_{13})$	$\varepsilon_{ST} = \frac{(\dot{E}_{12} + \dot{E}_{13})}{\dot{E}_6 + \dot{E}_{14} + \dot{W}_{AC}}$	38
absorber (AB)	$\dot{E}_D^{AB} = \dot{E}_1 + \dot{E}_{10} + \dot{Q}_{loss} \left(1 - \frac{T_0}{T_L}\right) - (\dot{E}_2 + \dot{E}_{11})$	$\varepsilon_{AB} = \frac{\dot{E}_2 + \dot{E}_{11} - \dot{Q}_{loss} \left(1 - \frac{T_0}{T_L}\right)}{\dot{E}_1 + \dot{E}_{10}}$	38
total plant (TOT)	$\dot{E}_D^{TOT} = \dot{E}_D^{FD} + \dot{E}_D^{PU} + \dot{E}_D^{TV} + \dot{E}_D^{HE} + \dot{E}_D^{AC} + \dot{E}_D^{ST} + \dot{E}_D^{AB} + \dot{E}_L^{AB}$	$\varepsilon_{TOT} = 1 - \frac{\dot{E}_D^{TOT}}{\dot{E}_F^{TOT}}$	

chemical exergy content of the hydrocarbon streams is 6025.33 MW, which almost remains unchanged during the absorption process. The conventional exergy analysis results are presented in Figure 4.

As observed in Figure 4, the greatest exergy destruction rate belongs to the stripper, 8.16 MW (43%). In this study, in addition to the lean amine, the separated acid gases are also referred to the stripper product as they can be sent to other gas refinery units for further treatment. The second destructive source, absorber, accounts for 7.56 MW (40%). It should be noted that the exergy destructions of the stripper and absorber are mainly influenced by the large steam/energy consumption ( $40.6 \text{ ton} \cdot \text{h}^{-1}$ ) and exothermic reactions, respectively. Based on the published literature, stripper and absorber are among the highest exergy destructive process components in AGR units.<sup>37,76</sup> For instance, Banat et al.<sup>39</sup> reported that the absorber has the greatest exergy destruction share (e.g., 25.84%) among all process components of the AGR unit. In another research study conducted by Ferrara et al.,<sup>76</sup> a stripper with 66% of total exergy destruction overtakes the remaining equipment of the AGR unit. Indeed, the heat of absorption reactions, released in the absorber, and the steam consumption in the regeneration section determine the magnitude of exergy destruction for each case study. Other process components are ranked in terms of exergy destruction, as follows: heat exchanger (1.33 MW, 7%), air cooler (1 MW, 5%), amine

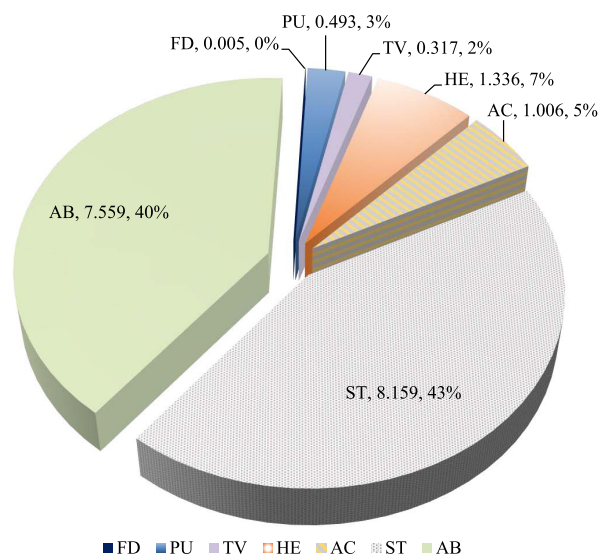


Figure 4. Exergy destruction of various equipment involved in the gas sweetening plant; exergy destruction values are reported in MW.

pump (0.49 MW, 3%), throttling valve (0.31 MW, 2%), and flash drum (0.0045 MW). The ranks for other process components are almost the same as those in the published research study;<sup>76</sup> however, the values of exergy destruction are

strongly a function of operation specifications (e.g., pressure, temperature, and composition). Therefore, this is not surprising to obtain different exergy destructions for the same process components at different operating conditions. Among all of the components, the flash drum has the lowest exergy destruction. Its marginal exergy destruction (0.0045 MW) can be ignored in the exergy efficiency calculation. Indeed, the flash drum is the physical vessel that separates gas from liquid phase based on a certain residence time; no heat or work is supplied to or consumed by this process component. Thus, a small exergy destruction is expected for the physical separation of the gas and liquid phases. The small exergy destruction of the flash drum in this study may differ from the values reported in other studies. In some research investigations, the throttling valve and flash drum are considered as a one-unit package that may result in a higher exergy destruction value than the current study.<sup>36,37,39</sup>

The exergy efficiency, as another indicator of exergy performance, is obtained to analyze the efficiency of the process components. Figure 5 illustrates the exergy efficiency of the AGR equipment.

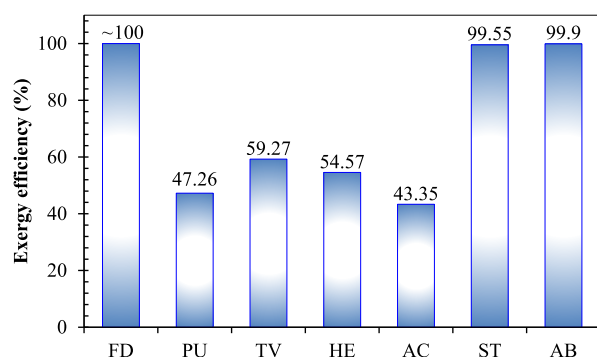


Figure 5. Magnitude of exergy efficiency for the process components.

The flash drum, stripper, and absorber are reported to exhibit the highest exergy efficiency. The high exergy performance of the flash drum is reasonable, considering its minor exergy destruction. The high exergy content of the absorber and stripper products leads to high exergy efficiencies that may falsify their performance interpretation. Note that both physical and chemical exergy values are involved in the exergy efficiency of these two process components. Thus, the small values of exergy destruction, compared to the input exergy, lead to high exergy efficiency. Note that excluding acid gas from the product streams and considering it as the exergy loss stream can significantly impact the stripper efficiency. The exergy efficiency of other process components such as amine pump (47.26%), throttling valve (59.27%), heat exchanger (54.57%), and air cooler (43.35%) is mainly influenced by physical exergy, and their exergy efficiencies are determined using the physical exergy. In this regard, the exergy destruction amounts are comparable to exergy values of fuel and product and offer more reasonable values. In general, exergy efficiency of process components is a weaker energy/exergy indicator than exergy destruction. This might be originated from the different characteristics of process components, which may involve physical, chemical, or the combination of both, in exergy efficiency calculation.

According to the conventional exergy analysis, the stripper, absorber, and heat exchanger have a higher potential for

performance enhancement, compared to the other process components. This conclusion is drawn based on the magnitudes of exergy destruction, revealing a significant extent of useful work is wasted at the operation state. The more exergy destruction shows higher potential to attain useful work.

**5.3. Advanced Exergy Analysis.** The main causes of thermodynamic imperfection and the possible ways for enhancement of the system components can be identified through an advanced exergy evaluation. However, the quantitative system irreversibility can be found by the conventional method. With the aid of advanced exergy analysis, the exergy destruction is split into two main groups: avoidable/unavoidable and endogenous/exogenous. Such a classification can better specify the sources of inefficiencies and facilitate feasible optimization of the system.

The avoidable exergy destruction in the advanced exergy assessment exhibits the amount of exergy that can be prevented from destruction due to technological constraints and equipment inefficiencies. The amounts of avoidable and unavoidable exergy destruction for each single equipment are provided in Figure 6.

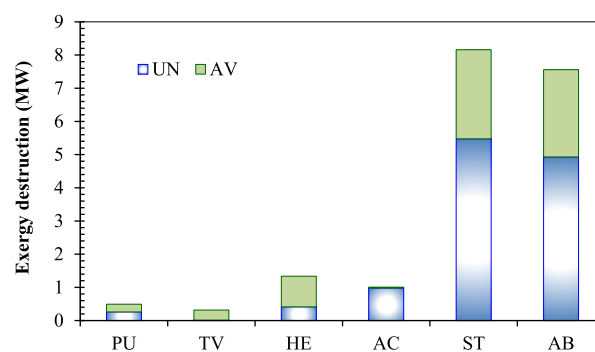


Figure 6. Avoidable and unavoidable exergy destruction values for the AGR unit.

Based on Figure 6, the avoidable exergy destruction values for the stripper, absorber, and heat exchanger are more significant than the corresponding unavoidable values. The highest avoidable exergy destruction (2.68 MW) belongs to the stripper, which is followed by the absorber with an avoidable exergy destruction of 2.63 MW. The improvement in the stripper can be achieved, considering a perfect heat transfer between the steam and rich amine stream. Since the boiler and stripper are considered as an integrated package, the advanced exergy analysis of the boiler is treated as a heat exchanger with the thermal limits, as summarized in Table 4. For the absorber, it is found that the hot side streams can be linked to the heat exchangers, to gain useful work or recover the heat loss over the absorption reactions.<sup>77</sup> The advanced and conventional exergy analyses represent the same ranks for the top three components (e.g., stripper, absorber, and heat exchanger) with the greatest potential of performance improvement. The amounts of avoidable exergy destruction for the stripper and absorber are approximately the same; these two equipment experience a considerable performance improvement, compared to the other process components. The second priority is given to the heat exchanger on the basis of the advanced exergy analysis. The remaining AGR equipment have a lower chance to be improved, considering the smaller potential of performance improvement based on avoidable exergy extent. However,



the throttling valve has the maximum relative potential improvement among the AGR process components. One can conclude that the entire exergy destruction of the throttling valve can be avoided if a turbo expander replaces the valve to generate mechanical work.<sup>78</sup> The throttling valve overtakes the amine pump and air cooler, considering its higher avoidable exergy destruction; this is not explored by the conventional exergy assessment. The significance of advanced exergy destruction is more highlighted for the air cooler; only a small improvement can be expected according to the advanced exergy evaluation, which is in contrast to the conventional exergy method. Indeed, the exergy destruction of the air cooler is mostly unavoidable exergy destruction. The main reason for this significant proportion of unavoidable exergy destruction to the overall exergy destruction (97.48%) is the heat loss to the atmosphere. This heat cannot be recovered as the temperature is not high enough to produce mechanical work. Olaleye and Wang<sup>38</sup> also reported the same exergy behavior for the air cooler.

The contribution of exogenous and endogenous exergy destruction extents is displayed in Figure 7. In fact,

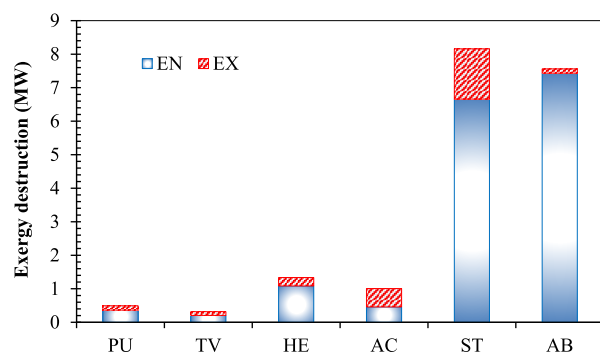


**Figure 7.** Endogenous (EN) and exogenous (EX) exergy destruction of different process components.

endogenous exergy destruction shows the equipment inter-connectivity. According to the literature, one can conclude that, mostly, the endogenous exergy destruction is higher than the exogenous exergy destruction.<sup>79,80</sup> High endogenous value means that the irreversibility is mainly originated from the process component itself. The air cooler is the only component with a higher exogenous exergy destruction, compared to its endogenous exergy value. This was also claimed by Olaleye and Wang.<sup>38</sup> The greater exogenous exergy destruction of the air cooler implies that other process components have a larger influence on the air cooler exergy destruction, compared to the impact of the air cooler on their performance. It should be noted the calculation of endogenous exergy destruction for the absorber and stripper is not an easy task because no ideal/theoretical condition can be identified/introduced for the chemical reactions. Thus, the absorber endogenous exergy destruction is obtained using the minimum liquid-to-gas ratio, which equals the least exergy destruction.<sup>38</sup> In addition, the stripper's total exergy destruction, excluding the boiler, is assumed to be endogenous.<sup>38</sup> The obtained exergy trends for the absorber and stripper are confirmed with the values/trends obtained by Olaleye and Wang.<sup>38</sup>

To achieve the realistic exergy efficiency, it is essential to exclude the exogenous exergy destruction imposed by the other process components. The high endogenous exergy

destructions belong to the absorber (7.43 MW), stripper (6.66 MW), and heat exchanger (1.08 MW). The endogenous exergy destruction provides a relatively similar trend, compared to the classical exergy evaluation and avoidable exergy destruction.

An advanced exergy analysis requires important exergy parameters, such as avoidable/exogenous, avoidable/endogenous, unavoidable/exogenous, and unavoidable/endogenous exergy destructions to achieve further practical recommendations/information on the process performance. Different types of exergy destructions for the plant equipment are depicted in Figure 8. As observed, the exergy destruction of the stripper

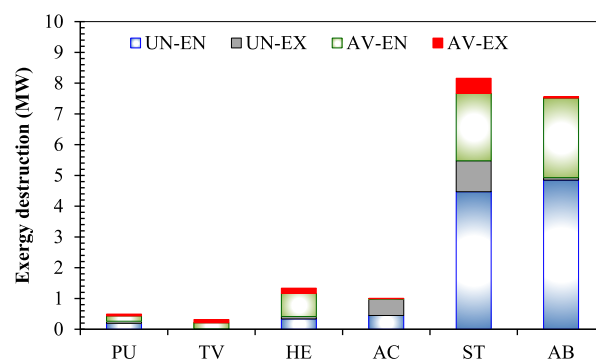


**Figure 8.** Contribution of various types of exergy destruction for each equipment.

and absorber is mainly due to unfavorable/endogenous destruction. However, a significant part of the total exergy destruction for these process components is avoidable/endogenous exergy destruction, revealing a high potential for operational improvement. More details on the advanced exergy destruction can be found in Table 8.

The avoidable/exogenous destruction is of great importance in the component efficiency. The avoidable/endogenous exergy destructions of all process components are remarkably larger than avoidable/exogenous values, excluding the air cooler. The higher magnitudes of avoidable/endogenous exergy destruction confirm the greater capability of the equipment to work at the optimal operating state. The avoidable/endogenous exergy destructions of the equipment in descending order are as follows: the absorber (2.58 MW), stripper (2.18 MW), heat exchanger (0.74 MW), throttling valve (0.19 MW), pump (0.17 MW), and air cooler (0.01 MW). Thus, the stripper and absorber need more attention/consideration as they can provide a better performance if the technological limitations are removed. The avoidable/endogenous values for the stripper, absorber, and heat exchanger reveal their high potential for efficiency enhancement. According to the advanced analysis, the total avoidable/endogenous exergy destruction (5.90 MW) is almost 6.5 times larger than avoidable/exogenous exergy destruction (0.89 MW). Likewise, the amount of unavoidable/endogenous exergy destruction surpasses unfavorable unavoidable/exogenous destruction.

Table 8 lists the amounts of various exergy destructions for all of the process components and the entire system.

The total plant efficiency on the basis of the conventional exergy evaluation is 99.70%. The plant efficiency in terms of modified exergy efficiency (i.e., excluding unavoidable and avoidable/exogenous exergy destruction) would be 99.90%.

Table 8. Advanced Exergy Analysis Results

component, $k$	$\dot{E}_{D,k}$ (MW)	$\dot{E}_{D,k}^{AV}$ (MW)	$\dot{E}_{D,k}^{UN}$ (MW)	$\dot{E}_{D,k}^{EN}$ (MW)	$\dot{E}_{D,k}^{EX}$ (MW)	$\dot{E}_{D,k}^{AV,EN}$ (MW)	$\dot{E}_{D,k}^{AV,EX}$ (MW)	$\dot{E}_{D,k}^{UN,EN}$ (MW)	$\dot{E}_{D,k}^{UN,EX}$ (MW)
FD	0.0045	0.0000	0.0045	0.0000	0.0045	0.0000	0.0000	0.0000	0.0045
PU	0.4931	0.2322	0.2609	0.3654	0.1277	0.1721	0.0601	0.1933	0.0676
TV	0.3166	0.3056	0.0110	0.2049	0.1117	0.1978	0.1079	0.0071	0.0039
HE	1.3356	0.9225	0.4131	1.0843	0.2513	0.7489	0.1736	0.3354	0.0777
AC	1.0062	0.0253	0.9809	0.4584	0.5478	0.0115	0.0138	0.4469	0.5340
ST	8.1590	2.6827	5.4763	6.6602	0.1498	2.1899	0.4928	4.4703	1.0060
AB	7.5591	2.6300	4.9291	7.4345	0.1247	2.5867	0.0434	4.8478	0.0813
total	18.874	6.7984	12.0758	16.2076	2.6666	5.9068	0.8916	10.3008	1.7750

Table 9. Performance Evaluation of Plant Using Classical and Advanced Exergy Analysis Parameters

component, $k$	$\varepsilon_k$ (%)	$\varepsilon_k^{\text{mod}}$ (%)	$y_{D,k}$ (%)	$y_{D,k}^{AV,EN}$ (%)	$\delta_k$ (%)	$\xi_k$ (%)	ERR <sub>k</sub> (%)	EIP <sub>k</sub> (%)
FD	99.99	100.00	0.0001	0.0000	0.0001	0.0001	0.0000	0.0005
PU	47.26	72.24	0.0078	0.0027	0.0051	0.0051	0.9117	34.115
TV	59.27	69.18	0.0050	0.0031	0.0019	0.0019	1.0479	15.622
HE	54.57	69.20	0.0212	0.0119	0.0093	0.0093	3.9680	19.438
AC	43.35	95.82	0.0160	0.0002	0.0158	0.0158	0.0610	54.312
ST	99.55	99.77	0.1292	0.0347	0.0945	0.0948	11.602	0.6358
AB	99.90	99.96	0.1197	0.0409	0.0787	0.0789	13.704	0.0689
Total	99.70	99.90	0.2988	0.0935	0.2053	0.2059	31.2959	0.2053

The latter value confirms the operation enhancement of the plant at the theoretical-unavoidable state. The high exergetic efficiency of the AGR unit implies the high exergy content of the product exergy value, mainly sweet gas. The natural gas has a high chemical exergy content that effectively influences the overall efficiency. Based on the results, the highest modified exergy performance is attributed to the flash drum (100%), absorber (99.96%), stripper (99.77%), and air cooler (95.82%). The large modified exergy efficiency of the air cooler comes from its small avoidable-endogenous exergy destruction. Also, a significant difference between the conventional and advanced exergy performance of the air cooler is observed, 43.35% compared to 95.82%. This high improvement comes from the air cooler significant unavoidable exergy destruction with respect to its avoidable destruction. In fact, the air cooler operates at its standard/optimal state and less possible improvement can be expected for this equipment. Thus, the priority for operation enhancement should be given to the other process equipment for attaining better operational performance. In other words, the avoidable exergy destruction of the air cooler (0.0115 MW) is smaller than the other process components. This observation acknowledges the importance of the advanced exergy assessment since the classical analysis may cause misleading interpretation and add an extra financial burden to the operating costs.

The performance assessment of the AGR unit is presented in Table 9. The leading contributors to the overall exergy destruction are in the similar order of the importance considering the exergy destruction ratio ( $y_{D,k}$ ): stripper (0.129), absorber (0.119), and heat exchanger (0.021). The sequence of the modified exergy destruction ratio is the same as the conventional one. Indeed, this parameter shows the exergy destruction quality. The modified exergy destruction ratio depends on the avoidable/exogenous exergy destruction value that mainly presents the actual potential of process improvement. As expected, the flash drum, air cooler, and amine pump exhibit the lowest modified exergy destruction ratio, since they are nearly at the optimal operation state. The exergetic fuel depletion ratio ( $\delta_k$ ) of the overall system is

0.2053. The stripper and absorber have the highest exergetic fuel depletion ratio, while the flash drum and throttling valve account for the minimum magnitudes of exergetic fuel depletion ratio. Indeed, the exergetic fuel depletion ratio indicates the possible enhancement percentage of the product by 0.205%, with respect to the total input fuel.

The same order is observed for the system components in terms of the exergetic productivity lack ratio ( $\xi_k$ ). This exergetic parameter is 0.2059% for the AGR unit, implying a 0.2059% reduction in the exergy consumption at the theoretical-unavoidable state of the plant. The exergetic rehabilitation ratio for the plant is 31.29%. According to Table 9, the high exergy rehabilitation ratio is attributed to the absorber (13.70%), stripper (11.60%), heat exchanger (3.9%), and valve (1.04%), respectively. It means that more priority should be given to the performance enhancement of the above process components since they can positively influence the total efficiency. The parameter of EIP<sub>k</sub> indicates the proportion of unrecoverable exergy destruction to the fuel exergy of the  $k^{\text{th}}$  component. This parameter is a proper measure to assess the operation of each component based on its input fuel. The reverse trend, compared to the exergy rehabilitation ratio, is expected for this parameter. The air cooler and pump have higher EIP<sub>k</sub> values of 54.31 and 34.11%, respectively, compared to other process components.

**5.4. Economic and Environmental Analysis.** In this section, the economic prospect of the AGR unit at the current state and unavoidable state (e.g., ignoring economical constraints; see Table 4), is taken into account. Figure 9 displays the individual costs and total expenses per year for the operation state and unavoidable state. According to Figure 9, the total costs decrease to nearly 22.7% while considering the unavoidable state. The electricity cost, carbon tax, and steam cost are reduced to 31.3, 21, and 20.1%, respectively.

Figure 10 demonstrates the calculated amount of CO<sub>2</sub> emissions and SEC index for the operation and unavoidable scenarios. As it is clear, the unavoidable mode experiences a considerable CO<sub>2</sub> emission reduction (21%), in comparison to the operational state. The SEC index of the unavoidable

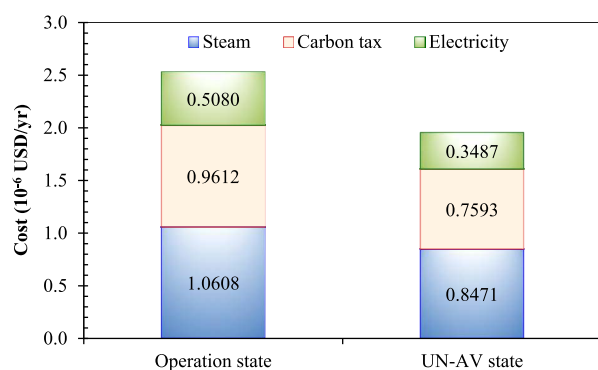


**Figure 9.** Individual and total costs for the operational state and unavoidable scenario.

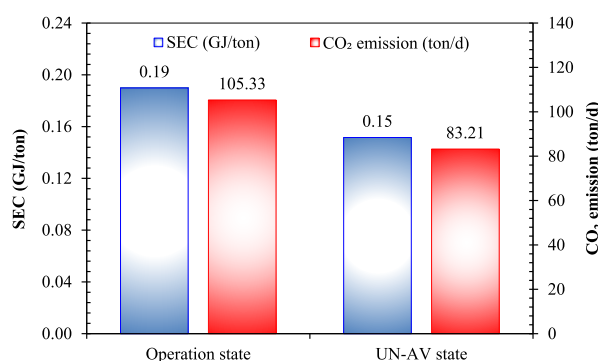


**Figure 10.** Magnitudes of SEC index and CO<sub>2</sub> emissions for the operation and unavoidable states.

scenario is substantially smaller than that of the real case. Thus, a 20.2% decrease in the SEC is obtained; this significant decrease in the SEC index is achieved because a smaller amount of steam is needed in the boiler, while dealing with the unavoidable mode.

The advanced exergy analysis, as a key tool for energy decision makers, can provide strategic guidelines for improving system efficiency. The presented advanced exergy analysis leads to obtaining new information that can be taken into account for AGR plants suffering from energy-consuming in various parts/units. Recognizing destruction sources and avoidable irreversibility can help to effectively increase the chance of attaining the optimal operating state. Implementation of efficient strategies for process component improvement in terms of exergy content would lead to saving a significant amount of energy and costs as well as mitigating significant GHG emissions.

The AGR unit's advanced exergy analysis encounters some major challenges. For instance, finding the theoretical/thermodynamic and unavoidable conditions for process equipment is not an easy task. The foundation of the advanced exergy analysis is to assume some key operating parameters at the ideal state where the technological constraints exist no longer. If these conditions cannot be found in the literature, one should consider a standard/logical magnitude for the unavoidable and theoretical states. Another major drawback in the advanced exergy evaluation is the need of a larger number of simulation/mathematical modeling runs, compared to the conventional exergy evaluation. On the other hand, an AGR unit with gigantic energy consumer elements requires the detailed energy/heat loss information of the equipment (e.g.,

absorber and stripper). In some cases, such information might not be available due to data confidentiality set by the industry/company.

The AGR unit can also be subjected to further advanced analysis such as exergoeconomic and exergoenvironmental assessment. Involvement of economic and environmental indexes in exergy destruction is of great importance that can further enrich the practicability and feasibility of exergy analysis. Utilization of hybridized advanced exergy analysis and energy optimization is also recommended for future research work. It is highly recommended to use a turbo expander instead of an expansion valve in the AGR unit. Also, using hot side streams from the absorber in the heat exchanger can significantly recover the heat loss and improve the unit energy/exergy efficiency. Similarly, hot side streams can be considered between the boiler and heat exchangers to prevent the heat loss in the stripping and to generate power. Another suggestion is to find an optimal solvent composition with the aid of an optimization algorithm through an advanced exergy analysis; this approach can substantially reduce the regeneration energy and sour gas removal efficiency.

## 6. SUMMARY AND CONCLUSIONS

In this study, an amine blend of MDEA–DEA–PZ is proposed for the acid gas removal through chemical/physical absorption. Removing CO<sub>2</sub> and H<sub>2</sub>S from natural gas is of great significance for gas cleaner production, considering various uses in homes and industries. To avoid health and safety concerns, the concentration of hydrogen sulfide and carbon dioxide should be reduced to the specific standard values. Hence, AGR unit has an undeniable role in sustainable and cleaner production of natural gas. On the other hand, AGR unit is an energy demand industrial sector that needs special care in terms of energy consumption minimization and GHG emission reduction. Energy and exergy analysis can provide effective tips/guidelines to better operate AGR units toward optimal performance. In this study, classical and advanced exergy analyses of an AGR unit are conducted to analyze the exergy efficiency of every process equipment and the entire system. To meet this objective, a robust simulation platform is introduced, which is validated by the real plant data. Considering MDEA–DEA–PZ as the new amine blend, this research offers valuable information in terms of process operation, energy conversion, and waste energy management. The main findings of the current study are presented below:

- The current AGR unit captures more than 96.6 and 99.7% of CO<sub>2</sub> and H<sub>2</sub>S, respectively. The steam consumption in the AGR unit is 40.6 ton·h<sup>−1</sup>, which is equal to 105.3 ton·day<sup>−1</sup> CO<sub>2</sub> emissions. The CO<sub>2</sub> emissions can be reduced to 83.2 ton·day<sup>−1</sup> if the current equipment are upgraded to the high-performance ones.
- A decrease in carbon tax payment would be an asset while implementing CO<sub>2</sub> reduction approaches. The carbon tax would decrease from 0.96 to 0.76 million USD/year, under unavoidable conditions.
- The electricity consumption lowers from 0.96 to 0.66 MW, while considering the unavoidable conditions.
- According to the classical exergy analysis, the exergy efficiency is 99.70% for the entire process, whereas the prediction obtained from the advanced exergy assessment is 99.90%.

- The conventional exergy assessment introduces the stripper (8.15 MW) with the highest exergy destruction amount. Also, 5.47 MW out of the overall exergy destruction accounts for the unavoidable exergy destruction. It implies that the potential for efficiency improvement of the stripper is high. In other words, the stripper has a high potential to work with better performance if the steam boiler works ideally in terms of heat generated from the steam for the rich amine stream.
- The second high exergy destruction source is the absorber. However, this process component exhibits a high potential for the operation improvement since nearly 65% of its exergy destruction can be prevented by removing technology constraints. The considerable heat of absorption reactions is mainly responsible for the massive exergy destruction occurred in the absorber. The exergy performance of the absorber would be elevated if the side streams are employed to lower the heat and to produce the mechanical work, consequently.
- The descending order of the avoidable/endogenous exergy destruction of the process components is as follows: absorber (2.58 MW), stripper (1.18 MW), heat exchanger (0.74 MW), throttling valve (0.19 MW), and pump (0.17 MW).
- In addition to the advanced exergy analysis, new exergetic terms are defined to explore how much the system operation can be enhanced. The exergetic productivity lack ratio, exergetic improvement potential, exergetic fuel depletion ratio, and exergetic rehabilitation ratio are 0.2059, 0.2053, 0.205, and 31.29%, respectively.
- The maximum exergy rehabilitation is obtained for the absorber (13.70%), confirming its high enhancement potential. The stripper with 11.60% exergy rehabilitation ratio holds the second rank, among the other equipment. This rank has been already confirmed by other exergetic parameters.
- The irreversibility sources resulted from interactions between the components of the AGR unit are included in the advanced exergy analysis. Thus, a more practical approach is developed through conducting an advanced exergy evaluation since the avoidable/unavoidable portions of the exergy destruction are identified. The advanced exergy assessment of gas sweetening plants provides process and operations engineers with practical tips/suggestions for process improvement.
- Enhancement of an AGR unit to the theoretical-unavoidable state needs upgraded equipment that may be currently unavailable, due to technological limitations. Another major challenge in energy optimization of the AGR unit is its dependency on high steam consumption in the regeneration section. The process optimization and utilization of new solvents/solvent blends may help to considerably lower energy consumption.
- This study could shed light on utilization of other solvents and new blends targeting the energy/exergy optimization of AGR unit.
- The proposed strategy in this study could be implemented on other thermal systems, in particular carbon capture processes. The current study can pave the way for an advanced and scientific assessment (e.g.,

exergoeconomic and technoeconomic) to investigate the economic aspect of AGR units as well.

## AUTHOR INFORMATION

### Corresponding Authors

**Mohamad Mohamadi-Baghmolaei** – Faculty of Engineering and Applied Science, Memorial University, St. John's, Newfoundland and Labrador A1B 3X7, Canada; Email: [m.mohammadibaghmolaei@mun.ca](mailto:m.mohammadibaghmolaei@mun.ca)

**Sohrab Zendehboudi** – Faculty of Engineering and Applied Science, Memorial University, St. John's, Newfoundland and Labrador A1B 3X7, Canada; [orcid.org/0000-0001-8527-9087](https://orcid.org/0000-0001-8527-9087); Email: [szendehboudi@mun.ca](mailto:szendehboudi@mun.ca)

### Authors

**Abdollah Hajizadeh** – Faculty of Engineering and Applied Science, Memorial University, St. John's, Newfoundland and Labrador A1B 3X7, Canada

**Xili Duan** – Faculty of Engineering and Applied Science, Memorial University, St. John's, Newfoundland and Labrador A1B 3X7, Canada; [orcid.org/0000-0001-5554-0758](https://orcid.org/0000-0001-5554-0758)

**Hodjat Shiri** – Faculty of Engineering and Applied Science, Memorial University, St. John's, Newfoundland and Labrador A1B 3X7, Canada

Complete contact information is available at: <https://pubs.acs.org/10.1021/acs.energyfuels.1c00590>

### Notes

The authors declare no competing financial interest.

## ACKNOWLEDGMENTS

The authors greatly appreciate the financial assistance received from Memorial University, Mitacs, and the Natural Sciences and Engineering Research Council of Canada (NSERC).

## NOMENCLATURES

### Acronyms

AB = absorber  
 AC = air cooler  
 AGR = acid gas removal  
 BRE = Bryan Research Engineering  
 COS = carbon sulfide  
 DEA = di-ethanolamine  
 DIPA = di-*iso*-propanolamine  
 DPD = dual-pressure low-temperature distillation  
 EIP = exergetic improvement potential ratio  
 ELECNRTL = electrolyte nonrandom two-liquid  
 ENRTL = electrolyte nonrandom two-liquid  
 EOS = equation of state  
 ERR = exergetic rehabilitation ratio  
 FD = flash drum  
 FJGRC = Fajr-e-Jam Gas Refining Company  
 GHG = greenhouse gas  
 HE = heat exchanger  
 IEA = International Energy Agency  
 LCA = life cycle assessment  
 LNG = liquified natural gas  
 LPG = liquified petroleum gas  
 LVC = lean vapor compression  
 MDEA = methyl-di-ethanolamine  
 MEA = mono-ethanolamine



MKUP = make up amine  
 MMSCMD = million standard cubic meters per day  
 PZ = piperazine  
 PU = pump  
 RD = relative deviation  
 RVC = rich vapor compression  
 SNG = synthesized natural gas  
 SRK = Soave–Redlich–Kwong  
 SEC = specific energy consumption  
 ST = stripper  
 TOT = total  
 TV = throttling valve

## VARIABLES/LETTERS

$a$  = activity  
 $d$  = derivative  
 $E$  = exergy, J  
 $\dot{E}$  = exergy flow, W  
 $ex$  = specific exergy, J·mol<sup>-1</sup>  
 $F$  = feed stream mass flow rate, ton·h<sup>-1</sup>  
 $g$  = gravity constant, m·s<sup>-2</sup>  
 $g_f$  = standard Gibbs free energy of formation, J·mol<sup>-1</sup>  
 $G$  = Gibbs free energy, J  
 $h$  = specific enthalpy, J·mol<sup>-1</sup>  
 $H$  = enthalpy, J  
 $L$  = loss stream mass flow rate, ton·h<sup>-1</sup>  
 $L/G$  = liquid-to-gas ratio  
 $M$  = molarity, mol·L<sup>-1</sup>  
 $n$  = number of moles, mole  
 $P$  = pressure, bar  
 $\Delta P$  = pressure difference, bar  
 $Q$  = heat, J  
 $\dot{Q}$  = heat flow, W  
 $R$  = gas constant, Pa·m<sup>3</sup>/mol·K  
 $s$  = specific entropy, J·mol<sup>-1</sup>·K<sup>-1</sup>  
 $S$  = entropy, J·K<sup>-1</sup>  
 $t$  = time, s  
 $T$  = temperature, K  
 $\Delta T$  = temperature difference, K  
 $U$  = internal energy, J  
 $V$  = fluid velocity, m·s<sup>-1</sup>  
 $W$  = work, J  
 $wt$  = weight percentage  
 $x$  = mole fraction (liquid state)  
 $y$  = mole fraction (gas state)  
 $y_D$  = exergy destruction ratio  
 $z$  = height, m  
 $Z$  = compressibility factor

## GREEK LETTERS

$\nu$  = stoichiometric coefficient  
 $\rho$  = molar density, mol·cm<sup>-3</sup>  
 $\delta$  = exergetic fuel depletion ratio  
 $\gamma$  = activity coefficient  
 $\eta$  = equipment efficiency  
 $\xi$  = exergetic productivity ratio  
 $\varepsilon$  = exergy efficiency  
 $\Psi$  = Murphree efficiency

## SUBSCRIPTS

0 = reference state  
 aq = aqueous

ch = chemical  
 D = destruction  
 f = formation  
 F = fuel  
 in = input  
 i, j = component  
 is = isentropic  
 $k$  = process component  
 L = loss  
 M = Murphree  
 min = minimum  
 mix = mixture  
 ph = physical  
 t = total  
 w = water  
 out = output  
 P = product  
 sol = solution  
 tot = total

## SUPERSCRIPTS

0 = standard state  
 a = aqueous state  
 AV = avoidable  
 EN = endogenous  
 EX = exogenous  
 ig = ideal gas  
 Op = operation  
 Sim = simulation  
 UN = unavoidable

## REFERENCES

- (1) Faramawy, S.; Zaki, T.; Sakr, A.-E. Natural gas origin, composition, and processing: A review. *J. Nat. Gas Sci. Eng.* **2016**, *34*, 34–54.
- (2) George, G.; Bhorla, N.; AlHallaq, S.; Abdala, A.; Mittal, V. Polymer membranes for acid gas removal from natural gas. *Sep. Purif. Technol.* **2016**, *158*, 333–356.
- (3) Beyca, O. F.; Ervural, B. C.; Tatoglu, E.; Ozuyar, P. G.; Zaim, S. Using machine learning tools for forecasting natural gas consumption in the province of Istanbul. *Energy Econ.* **2019**, *80*, 937–949.
- (4) British Petroleum statistical review of world energy, 2013; p 48. <http://large.stanford.edu/courses/2013/ph240/lim1/docs/bpreview.pdf>.
- (5) British Petroleum energy outlook 2035, 2014. <https://www.bp.com/en/global/corporate/news-and-insights/press-releases/energy-outlook-2035.html>.
- (6) Bloomberg New Energy Finance. *New Energy Outlook Executive Summary*; Technical Report, 2017. <https://www.actu-environnement.com/media/pdf>.
- (7) MohamadiBaghmolaie, M.; Mahmoudy, M.; Jafari, D.; MohamadiBaghmolaie, R.; Tabkhi, F. Assessing and optimization of pipeline system performance using intelligent systems. *J. Nat. Gas Sci. Eng.* **2014**, *18*, 64–76.
- (8) MohamadiBaghmolaie, M.; Tabkhi, F.; Sargolzaei, J. Exergetic approach to investigate the arrangement of compressors of a pipeline boosting station. *Energy Technol.* **2014**, *2*, 732–741.
- (9) Mokhatab, S.; Poe, W. A.; Mak, J. Y. *Handbook of Natural Gas Transmission and Processing: Principles and Practices*, 4th ed.; Gulf Professional Publishing, 2018; p 862.
- (10) Huguet, E.; Coq, B.; Durand, R.; Leroi, C.; Cadours, R.; Hulea, V. A highly efficient process for transforming methyl mercaptan into hydrocarbons and H<sub>2</sub>S on solid acid catalysts. *Appl. Catal., B* **2013**, *134–135*, 344–348.
- (11) Abotaleb, A.; El-Naas, M. H.; Amhamed, A. Enhancing gas loading and reducing energy consumption in acid gas removal

systems: A simulation study based on real NGL plant data. *J. Nat. Gas Sci. Eng.* **2018**, *55*, 565–574.

(12) Yi, S.; Ma, X.; Pinnau, I.; Koros, W. J. A high-performance hydroxyl-functionalized polymer of intrinsic microporosity for an environmentally attractive membrane-based approach to decontamination of sour natural gas. *J. Mater. Chem. A* **2015**, *3*, 22794–22806.

(13) Taheri, M.; Mohebbi, A.; Hashemipour, H.; Rashidi, A. M. Simultaneous absorption of carbon dioxide (CO<sub>2</sub>) and hydrogen sulfide (H<sub>2</sub>S) from CO<sub>2</sub>–H<sub>2</sub>S–CH<sub>4</sub> gas mixture using amine-based nanofluids in a wetted wall column. *J. Nat. Gas Sci. Eng.* **2016**, *28*, 410–417.

(14) Rufford, T. E.; Smart, S.; Watson, G. C.; Graham, B.; Boxall, J.; Da Costa, J. D.; May, E. The removal of CO<sub>2</sub> and N<sub>2</sub> from natural gas: A review of conventional and emerging process technologies. *J. Pet. Sci. Eng.* **2012**, *94*–95, 123–154.

(15) Øi, L. E.; Bråthen, T.; Berg, C.; Brekne, S. K.; Flatin, M.; Johnsen, R.; Moen, I. G.; Thomassen, E. Optimization of configurations for amine based CO<sub>2</sub> absorption using Aspen HYSYS. *Energy Procedia* **2014**, *51*, 224–233.

(16) Zhang, F.; Shen, B.; Sun, H.; Liu, J.; Liu, L. Rational formulation design and commercial application of a new hybrid solvent for selectively removing H<sub>2</sub>S and organosulfurs from sour natural gas. *Energy Fuels* **2016**, *30*, 12–19.

(17) Kohl, A.; Nielsen, R. *Gas Purification*, 5th ed.; Gulf Professional Publishing, 1997; p 900.

(18) Nguyen, T.; Hilliard, M.; Rochelle, G. T. Amine volatility in CO<sub>2</sub> capture. *Int. J. Greenhouse Gas Control* **2010**, *4*, 707–715.

(19) Nguyen, T.; Hilliard, M.; Rochelle, G. Volatility of aqueous amines in CO<sub>2</sub> capture. *Energy Procedia* **2011**, *4*, 1624–1630.

(20) El Hadri, N.; Quang, D. V.; Goetheer, E. L.; Zahra, M. R. A. Aqueous amine solution characterization for post-combustion CO<sub>2</sub> capture process. *Appl. Energy* **2017**, *185*, 1433–1449.

(21) Rochelle, G.; Chen, E.; Freeman, S.; Van Wagener, D.; Xu, Q.; Voice, A. Aqueous piperazine as the new standard for CO<sub>2</sub> capture technology. *Chem. Eng. J.* **2011**, *171*, 725–733.

(22) Goff, G. S.; Rochelle, G. T. Monoethanolamine degradation: O<sub>2</sub> mass transfer effects under CO<sub>2</sub> capture conditions. *Ind. Eng. Chem. Res.* **2004**, *43*, 6400–6408.

(23) Veltman, K.; Singh, B.; Hertwich, E. G. Human and environmental impact assessment of postcombustion CO<sub>2</sub> capture focusing on emissions from amine-based scrubbing solvents to air. *Environ. Sci. Technol.* **2010**, *44*, 1496–1502.

(24) Chakravarty, T.; Phukan, U.; Weiland, R. Reaction of acid gases with mixtures of amines. *Chem. Eng. Prog.* **1985**, *81*, 32–36.

(25) Dash, S. K.; Samanta, A.; Samanta, A. N.; Bandyopadhyay, S. S. Vapour liquid equilibria of carbon dioxide in dilute and concentrated aqueous solutions of piperazine at low to high pressure. *Fluid Phase Equilib.* **2011**, *300*, 145–154.

(26) Moiola, S.; Pellegrini, L. A.; Romano, M. C.; Giuffrida, A. Pre-combustion CO<sub>2</sub> removal in IGCC plant by MDEA scrubbing: modifications to the process flowsheet for energy saving. *Energy Procedia* **2017**, *114*, 2136–2145.

(27) Aromada, S. A.; Øi, L. E. Energy and Economic Analysis of Improved Absorption Configurations for CO<sub>2</sub> Capture. *Energy Procedia* **2017**, *114*, 1342–1351.

(28) Hatmi, K. A.; Mashrafi, A. A.; Balushi, S. U. A.; Al-Kalbani, H.; Al-Battashi, M.; Shaikh, M. In *Energy Savings of Amine Sweetening Process through Lean and Rich Vapor Compression Approaches*, Abu Dhabi International Petroleum Exhibition & Conference, 2018; Society of Petroleum Engineers; Society of Petroleum Engineers, 2018.

(29) Law, L. C.; Azudin, N. Y.; Shukor, S. R. A. Optimization and economic analysis of amine-based acid gas capture unit using monoethanolamine/methyl diethanolamine. *Clean Technol. Environ. Policy* **2018**, *20*, 451–461.

(30) Gutierrez, J. P.; Tarifa, E. E.; Erdmann, E. Steady-state energy optimization and transition assessment in a process of CO<sub>2</sub> absorption from natural gas. *Energy* **2018**, *159*, 1016–1023.

(31) Abd, A. A.; Naji, S. Z.; Barifcani, A. Comprehensive evaluation and sensitivity analysis of regeneration energy for acid gas removal plant using single and activated-methyl diethanolamine solvents. *Chin. J. Chem. Eng.* **2020**, *28*, 1684–1693.

(32) Baghmolaie, M.; Tabkhi, F. Operation analysis of rotary tools of compressor station using exergy approach. *Int. J. Eng.* **2014**, *27*, 1815–1822.

(33) Szargut, J.; Morris, D. R.; Steward, F. R. *Exergy Analysis of Thermal, Chemical, and Metallurgical Processes*, 1st ed.; Hemisphere, 1987.

(34) Koroneos, C.; Spachos, T.; Moussiopoulos, N. Exergy analysis of renewable energy sources. *Renewable Energy* **2003**, *28*, 295–310.

(35) Mohamadi-Baghmolaie, M.; Hajizadeh, A.; Zahedizadeh, P.; Azin, R.; Zendehboudi, S. Evaluation of hybridized performance of amine scrubbing plant based on exergy, energy, environmental, and economic prospects: A gas sweetening plant case study. *Energy* **2021**, *214*, No. 118715.

(36) Lee, W.-S.; Lee, J.-C.; Oh, H.-T.; Baek, S.-W.; Oh, M.; Lee, C.-H. Performance, economic and exergy analyses of carbon capture processes for a 300 MW class integrated gasification combined cycle power plant. *Energy* **2017**, *134*, 731–742.

(37) Feyzi, V.; Beheshti, M.; Kharaji, A. G. Exergy analysis: A CO<sub>2</sub> removal plant using a-MDEA as the solvent. *Energy* **2017**, *118*, 77–84.

(38) Olaleye, A. K.; Wang, M. Conventional and advanced exergy analysis of post-combustion CO<sub>2</sub> capture based on chemical absorption integrated with supercritical coal-fired power plant. *Int. J. Greenhouse Gas Control* **2017**, *64*, 246–256.

(39) Banat, F.; Younas, O.; Didarul, I. Energy and exergetic dissection of a natural gas sweetening plant using methyldiethanol amine (MDEA) solution. *J. Nat. Gas Sci. Eng.* **2014**, *16*, 1–7.

(40) Nejat, T.; Movasati, A.; Wood, D. A.; Ghanbarabadi, H. Simulated exergy and energy performance comparison of physical–chemical and chemical solvents in a sour gas treatment plant. *Chem. Eng. Res. Des.* **2018**, *133*, 40–54.

(41) Mehdizadeh-Fard, M.; Pourfayaz, F. Advanced exergy analysis of heat exchanger network in a complex natural gas refinery. *J. Cleaner Prod.* **2019**, *206*, 670–687.

(42) Hajizadeh, A.; Mohamadi-Baghmolaie, M.; Azin, R.; Osfour, S.; Heydari, I. Technical and economic evaluation of flare gas recovery in a giant gas refinery. *Chem. Eng. Res. Des.* **2018**, *131*, 506–519.

(43) Rocco, M. V.; Langè, S.; Pigoli, L.; Colombo, E.; Pellegrini, L. A. Assessing the energy intensity of alternative chemical and cryogenic natural gas purification processes in LNG production. *J. Cleaner Prod.* **2019**, *208*, 827–840.

(44) Zeng, S.; Gu, J.; Yang, S.; Zhou, H.; Qian, Y. Comparison of techno-economic performance and environmental impacts between shale gas and coal-based synthetic natural gas (SNG) in China. *J. Cleaner Prod.* **2019**, *215*, 544–556.

(45) Safari, A.; Vesali-Naseh, M. Design and optimization of hydrodesulfurization process for liquefied petroleum gases. *J. Cleaner Prod.* **2019**, *220*, 1255–1264.

(46) Hashemi, M.; Pourfayaz, F.; Mehrpooya, M. Energy, exergy, exergoeconomic and sensitivity analyses of modified Claus process in a gas refinery sulfur recovery unit. *J. Cleaner Prod.* **2019**, *220*, 1071–1087.

(47) Abkhiz, V.; Heydari, I. Comparison of amine solutions performance for gas sweetening. *Asia-Pac. J. Chem. Eng.* **2014**, *9*, 656–662.

(48) Rodríguez, N.; Mussati, S.; Scenna, N. Optimization of post-combustion CO<sub>2</sub> process using DEA–MDEA mixtures. *Chem. Eng. Res. Des.* **2011**, *89*, 1763–1773.

(49) Plaza, J. M.; Rochelle, G. T. Modeling pilot plant results for CO<sub>2</sub> capture by aqueous piperazine. *Energy Procedia* **2011**, *4*, 1593–1600.

(50) Kidnay, A. J.; Parrish, W. R.; McCartney, D. G. *Fundamentals of Natural Gas Processing*, 3rd ed.; CRC Press, 2019.

(51) Stewart, M.; Arnold, K. *Gas Sweetening and Processing Field Manual*, 3rd ed.; Gulf Professional Publishing, 2011; p 200.

- (52) Sheilan, M. H.; Spooner, B. H.; van Hoorn, E.; Street, D.; Sames, J. A. *Amine Treating and Sour Water Stripping*, 5th ed.; Amine Experts, 2008; p 520.
- (53) Caplow, M. Kinetics of carbamate formation and breakdown. *J. Am. Chem. Soc.* **1968**, *90*, 6795–6803.
- (54) Derks, P.; Kleingeld, T.; Van Aken, C.; Hogendoorn, J.; Versteeg, G. Kinetics of absorption of carbon dioxide in aqueous piperazine solutions. *Chem. Eng. Sci.* **2006**, *61*, 6837–6854.
- (55) Sun, W.-C.; Yong, C.-B.; Li, M.-H. Kinetics of the absorption of carbon dioxide into mixed aqueous solutions of 2-amino-2-methyl-1-propanol and piperazine. *Chem. Eng. Sci.* **2005**, *60*, 503–516.
- (56) Ermatchkov, V.; Kamps, A.P.-S.; Maurer, G. Chemical equilibrium constants for the formation of carbamates in (carbon dioxide+ piperazine+ water) from 1H-NMR-spectroscopy. *J. Chem. Thermodyn.* **2003**, *35*, 1277–1289.
- (57) Bishnoi, S.; Rochelle, G. T. Absorption of carbon dioxide into aqueous piperazine: reaction kinetics, mass transfer and solubility. *Chem. Eng. Sci.* **2000**, *55*, 5531–5543.
- (58) Haghtalab, A.; Izadi, A.; Shojaeian, A. High pressure measurement and thermodynamic modeling the solubility of H<sub>2</sub>S in the aqueous N-methyldiethanolamine+ 2-amino-2-methyl-1-propanol + piperazine systems. *Fluid Phase Equilib.* **2014**, *363*, 263–275.
- (59) Cengel, Y.; Boles, M. A. *Thermodynamics: An Engineering Approach*, 4th ed.; McGraw-Hill, 2002; p 890.
- (60) Szargut, J. The potential balance of chemical processes. *Arch. Budowy Masz.* **1957**, *4*, 89–117.
- (61) Szargut, J. Exergy balance of metallurgical processes. *Arch. Hutn.* **1961**, *6*, 23–60.
- (62) Tsatsaronis, G.; Park, M.-H. On avoidable and unavoidable exergy destructions and investment costs in thermal systems. *Energy Convers. Manage.* **2002**, *43*, 1259–1270.
- (63) Kelly, S.; Tsatsaronis, G.; Morosuk, T. Advanced exergetic analysis: Approaches for splitting the exergy destruction into endogenous and exogenous parts. *Energy* **2009**, *34*, 384–391.
- (64) Sayadi, S.; Tsatsaronis, G.; Morosuk, T. Splitting the dynamic exergy destruction within a building energy system into endogenous and exogenous parts using measured data from the building automation system. *Int. J. Energy Res.* **2020**, *44*, 4395–4410.
- (65) Yamankaradeniz, N. Thermodynamic performance assessments of a district heating system with geothermal by using advanced exergy analysis. *Renewable Energy* **2016**, *85*, 965–972.
- (66) Tsatsaronis, G.; Czesla, F. Thermoeconomics. In *Encyclopedia of Physical Science and Technology*, 3rd ed.; Meyers, R., Ed.; Academic Press: New York, 2002; Vol. 16, pp 659–680.
- (67) Morosuk, T.; Tsatsaronis, G. Advanced exergy-based methods used to understand and improve energy-conversion systems. *Energy* **2019**, *169*, 238–246.
- (68) Mohammadi, Z.; Fallah, M.; Mahmoudi, S. S. Advanced exergy analysis of recompression supercritical CO<sub>2</sub> cycle. *Energy* **2019**, *178*, 631–643.
- (69) Mehrpooya, M.; Lazemzade, R.; Sadaghiani, M. S.; Parishani, H. Energy and advanced exergy analysis of an existing hydrocarbon recovery process. *Energy Convers. Manage.* **2016**, *123*, 523–534.
- (70) McCabe, W. L.; Smith, J. C.; Harriott, P. *Unit Operations of Chemical Engineering*, 2nd ed.; McGraw-Hill: New York, 1967; Vol. 5, p 1007.
- (71) Office, C. B. Impose a Tax on Emissions of Greenhouse Gases, 2018. <https://www.cbo.gov/budget-options/2018/54821> (June 25).
- (72) Administration, E. I. Natural Gas Prices, 2019. [https://www.eia.gov/dnav/ng/ng\\_pri\\_sum\\_dcu\\_nus\\_m.htm](https://www.eia.gov/dnav/ng/ng_pri_sum_dcu_nus_m.htm) (June 25).
- (73) Talebizadehsardari, P.; Ehyaei, M.; Ahmadi, A.; Jamali, D.; Shirmohammadi, R.; Eyvazian, A.; Ghasemi, A.; Rosen, M. A. Energy, exergy, economic, exergoeconomic, and exergoenvironmental (SE) analyses of a triple cycle with carbon capture. *J. CO<sub>2</sub> Util.* **2020**, *41*, No. 101258.
- (74) Mehrpooya, M.; Ansarinassab, H. Exergoeconomic evaluation of single mixed refrigerant natural gas liquefaction processes. *Energy Convers. Manage.* **2015**, *99*, 400–413.
- (75) Khosravi, H.; Salehi, G. R.; Azad, M. T. Design of structure and optimization of organic Rankine cycle for heat recovery from gas turbine: The use of 4E, advanced exergy and advanced exergoeconomic analysis. *Appl. Therm. Eng.* **2019**, *147*, 272–290.
- (76) Ferrara, G.; Lanzini, A.; Leone, P.; Ho, M.; Wiley, D. Exergetic and exergoeconomic analysis of post-combustion CO<sub>2</sub> capture using MEA-solvent chemical absorption. *Energy* **2017**, *130*, 113–128.
- (77) Bhattacharyya, D.; Miller, D. C. Post-combustion CO<sub>2</sub> capture technologies—a review of processes for solvent-based and sorbent-based CO<sub>2</sub> capture. *Curr. Opin. Chem. Eng.* **2017**, *17*, 78–92.
- (78) Qyyum, M. A.; Ali, W.; Long, N. V. D.; Khan, M. S.; Lee, M. Energy efficiency enhancement of a single mixed refrigerant LNG process using a novel hydraulic turbine. *Energy* **2018**, *144*, 968–976.
- (79) Ochoa, G. V.; Prada, G.; Duarte-Forero, J. Carbon footprint analysis and advanced exergo-environmental modeling of a waste heat recovery system based on a recuperative organic Rankine cycle. *J. Cleaner Prod.* **2020**, No. 122838.
- (80) Gholamian, E.; Hanafizadeh, P.; Ahmadi, P. Advanced exergy analysis of a carbon dioxide ammonia cascade refrigeration system. *Appl. Therm. Eng.* **2018**, *137*, 689–699.